



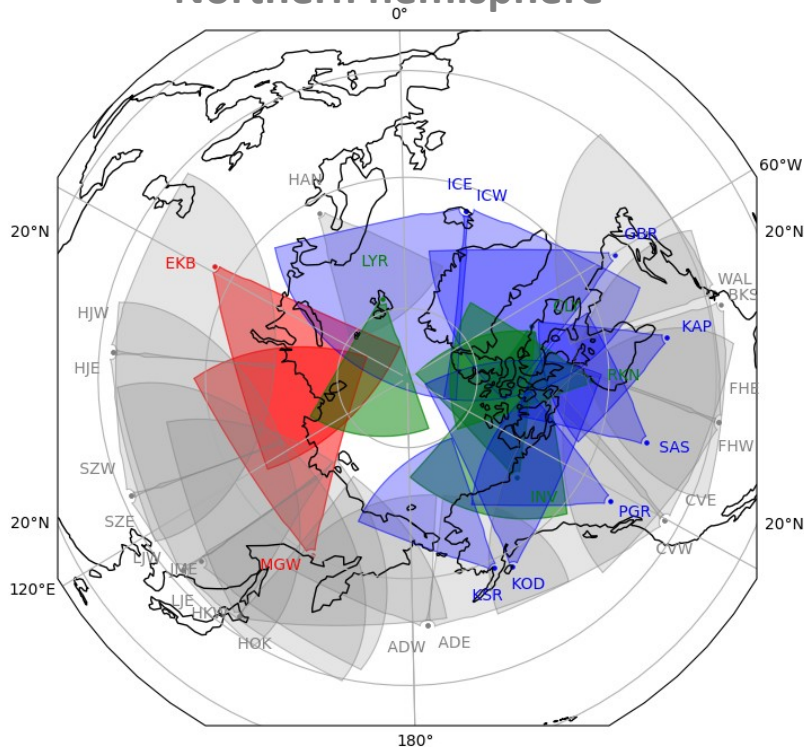
STUDY OF IONOSPHERIC IRREGULARITIES BASED ON HF RADAR NETWORK DATA

Alexey V. Oinats

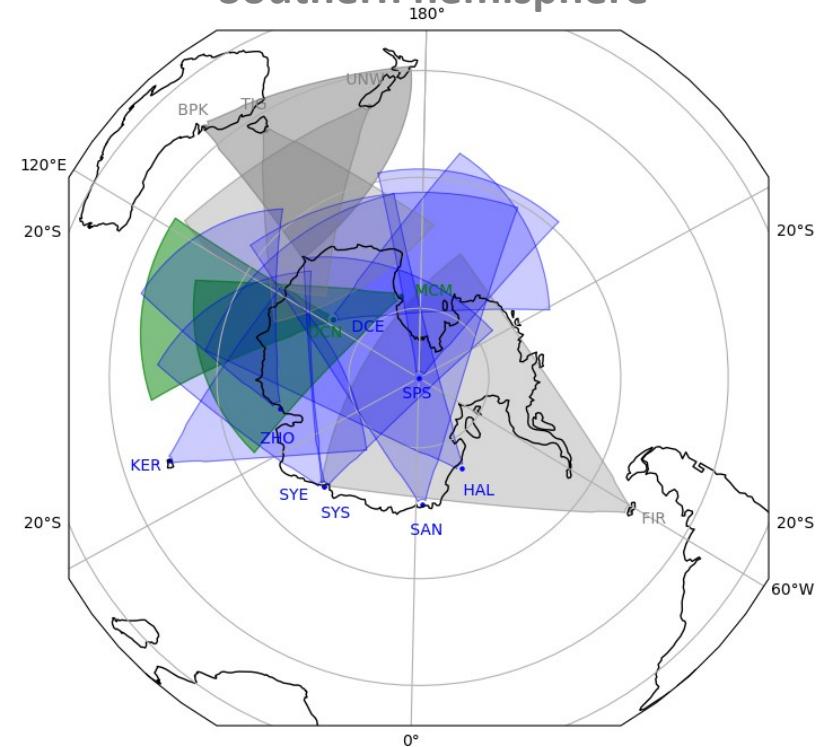
Institute of Solar-Terrestrial Physics SB RAS, Irkutsk, Russia

oinats@iszf.irk.ru

Northern hemisphere



Southern hemisphere



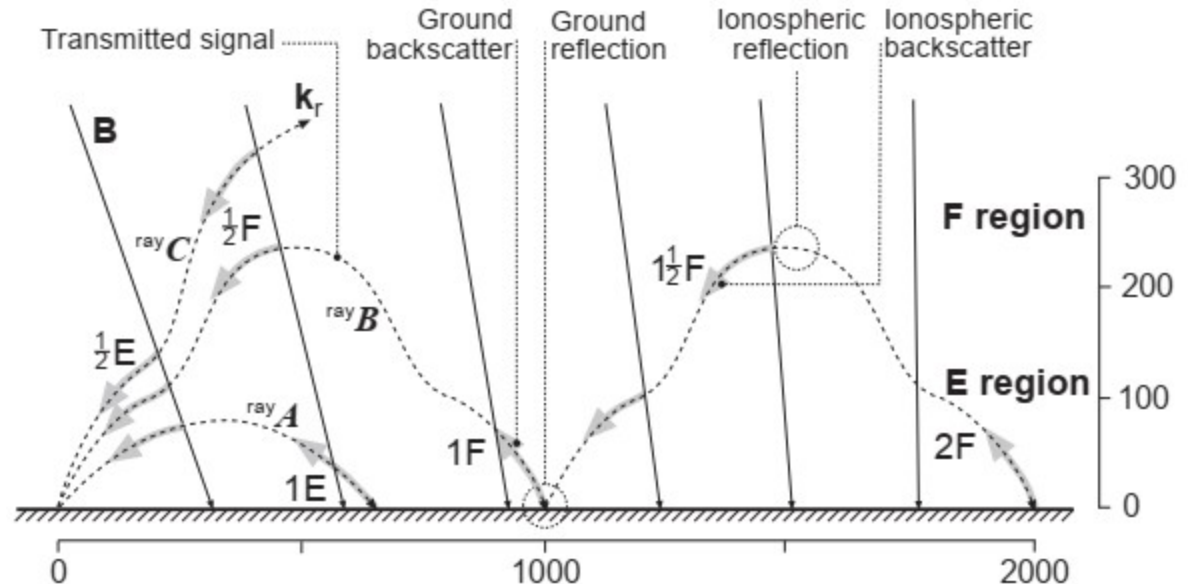
OUTLINE

INTRODUCTION

1. Medium scale traveling ionospheric disturbances (MSTIDs)
 - 1.1. TID's parameters determination technique
 - 1.2. Statistical study of MSTID's parameters
 - 1.3. Comparison with neutral wind model (HWM14)
2. Field-aligned irregularities (FAI). GDI growth rate
 - 2.1. FAI observation during St.Patrick superstorm (March 17-18, 2015). Comparison with GSMTIP
 - 2.2. Statistical study of FAI occurrence observed by EKB and MGW radars
 - 2.3. Comparison with empirical ionosphere models

CONCLUSIONS and FINAL REMARKS

HF WAVES PROPAGATION MODES (3-30 MHz)



INTRODUCTION

Russian HF radars

Operational frequency: 8-20 MHz

Number of beams: 16

Beam width: $\sim 3.5^\circ$

Beam separation angle: 3.24°

Field-of-view: $\sim 52^\circ$

Range gate: 15/45 km

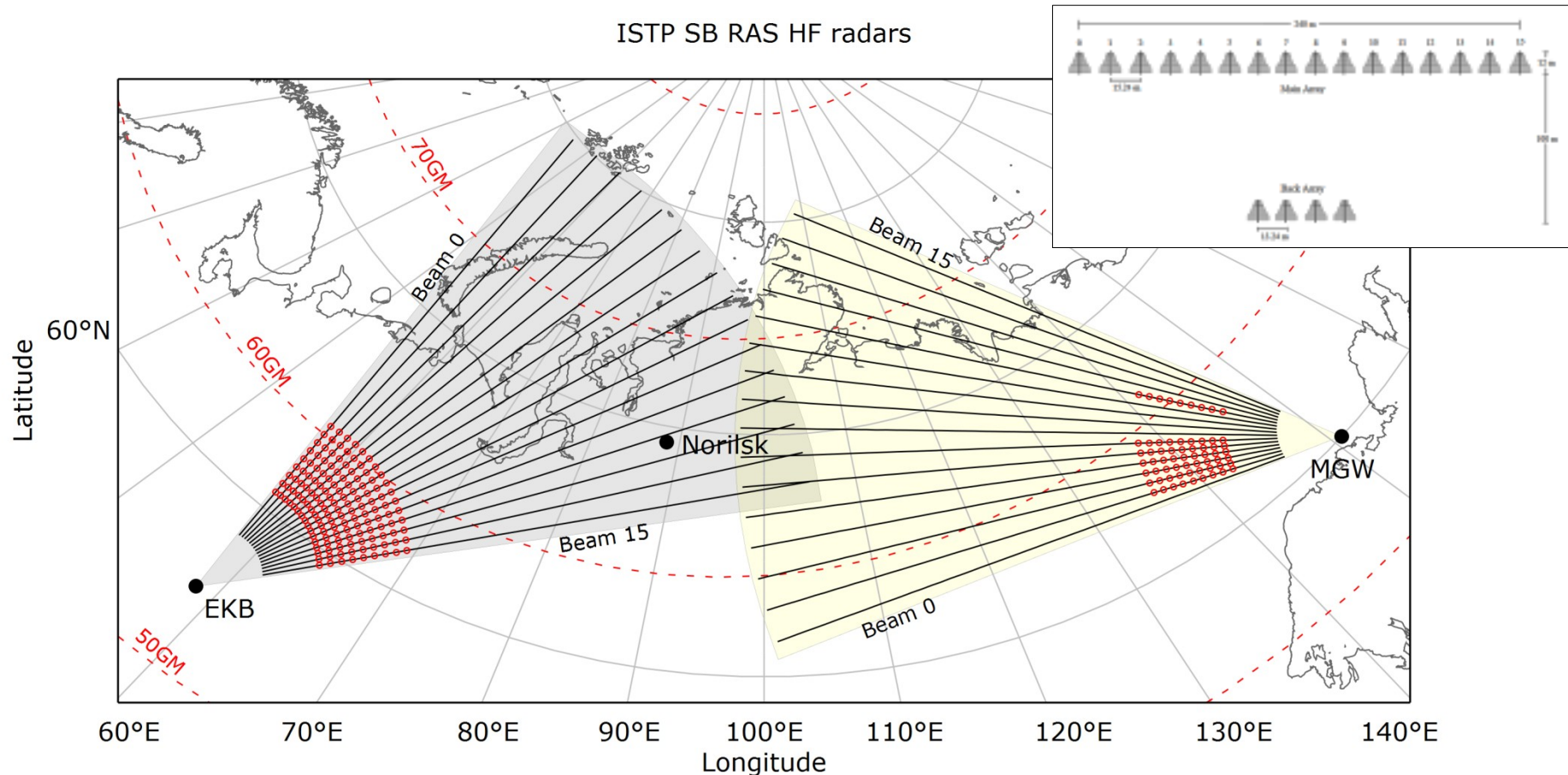
Stereo mode – 2 channels

First light dates

EKB: December 2012

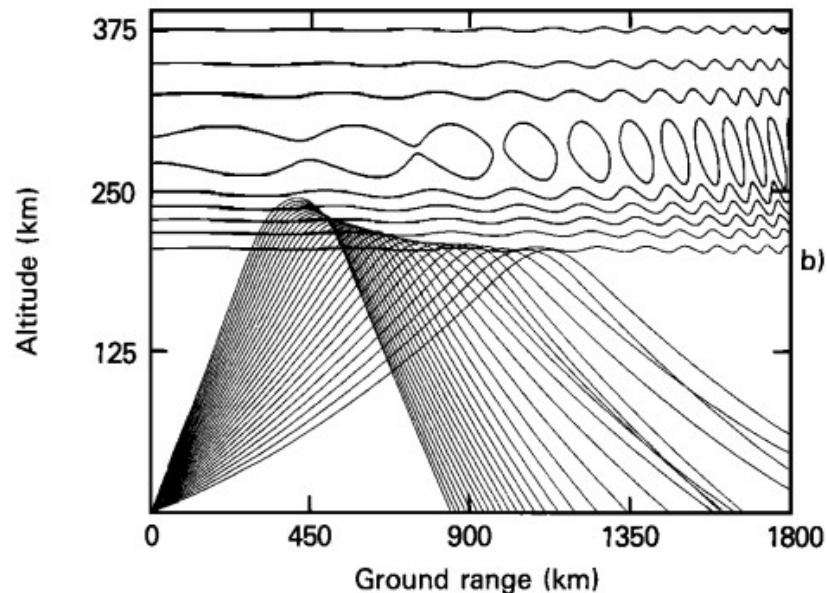
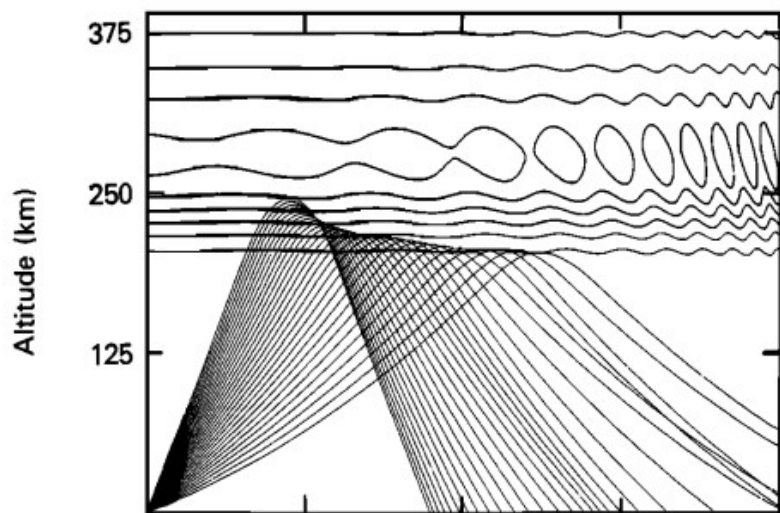
MGW: October 2020

Phased array antenna



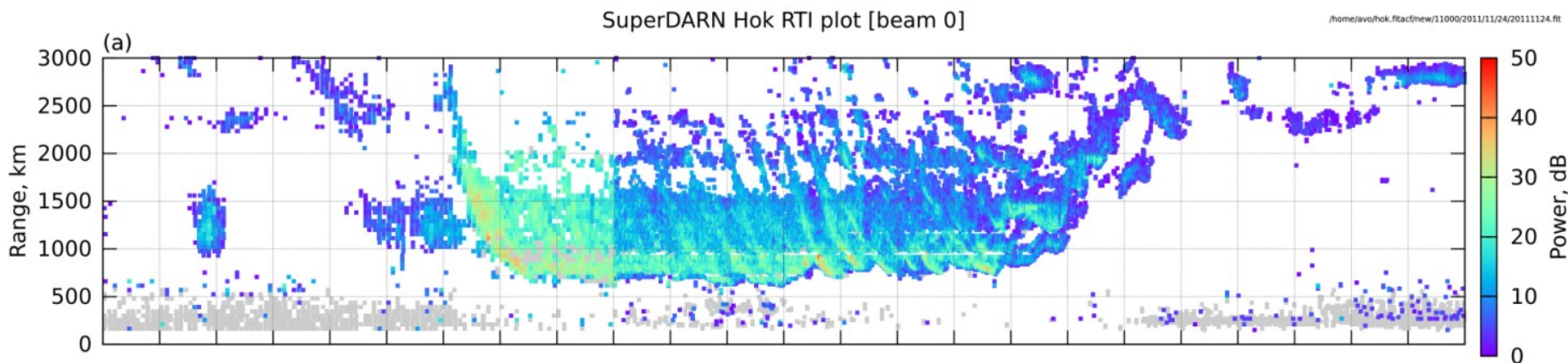
1. Medium scale traveling ionospheric disturbances (MSTIDs)

Simulation example



Observation

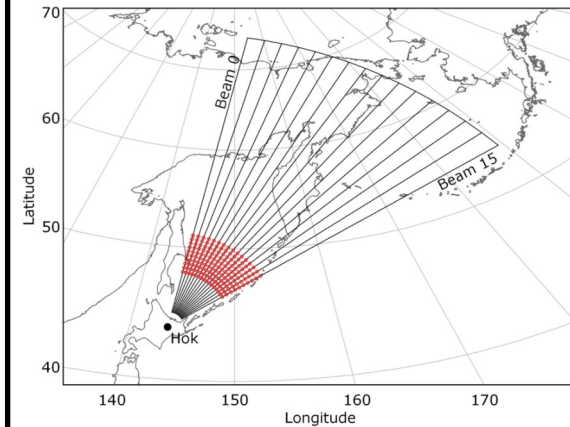
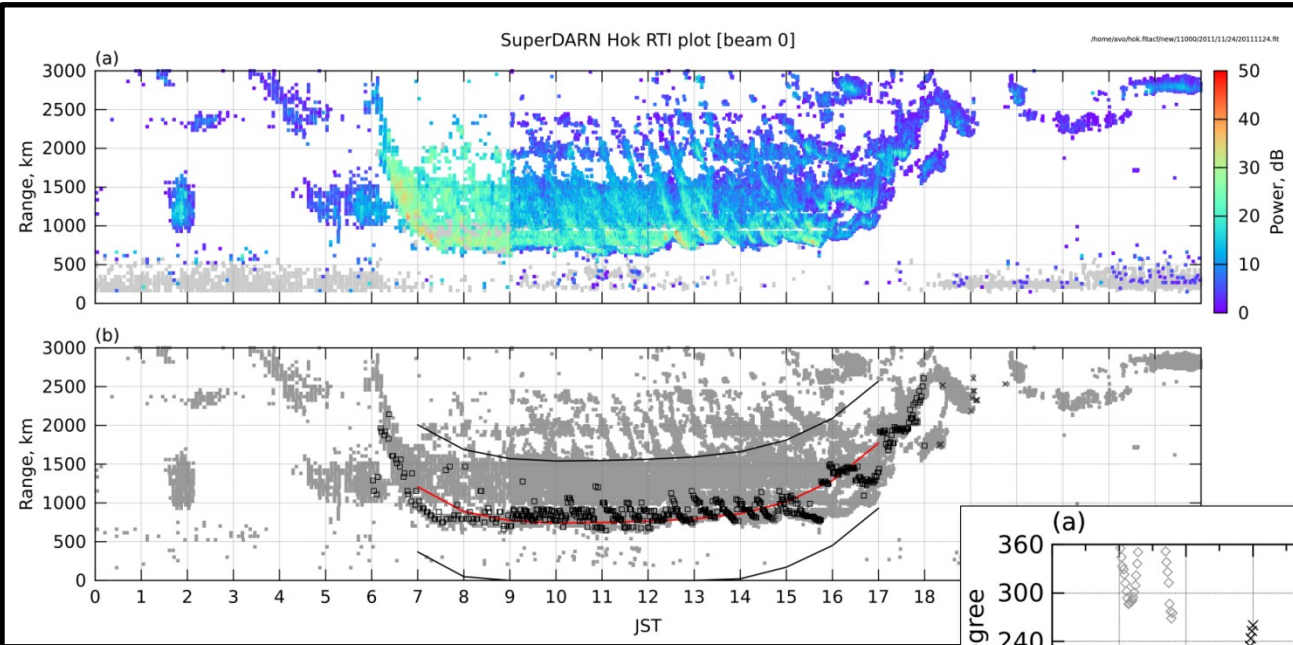
Samson et al. (1990)



Oinats et al. (2015)

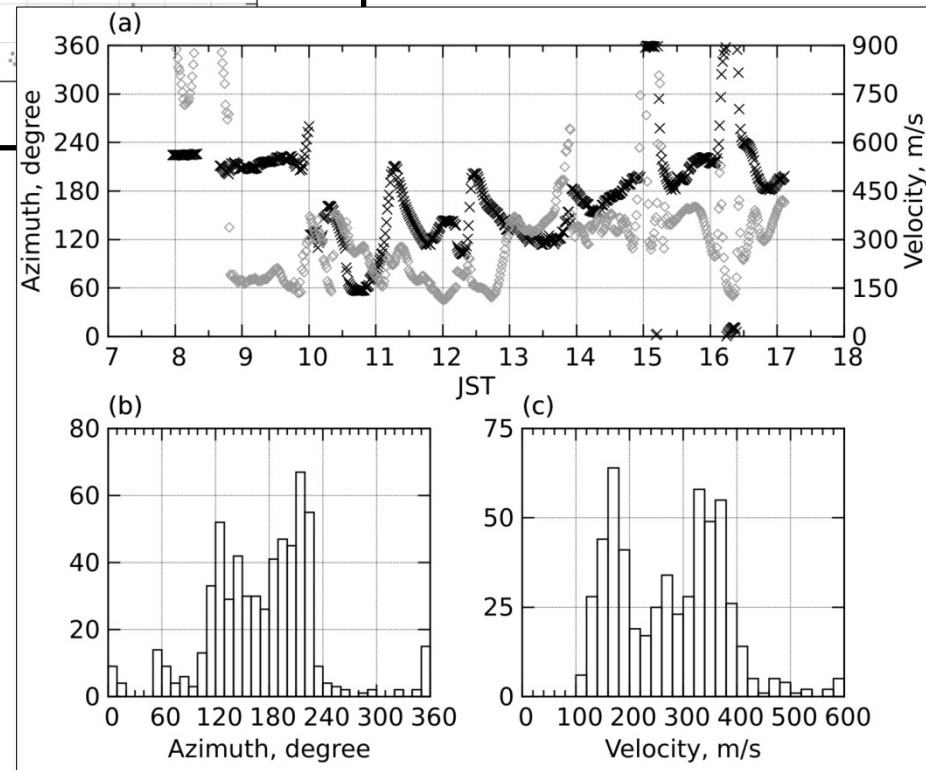
1.1. TID's parameters determination technique

Oinats et al. (2015)

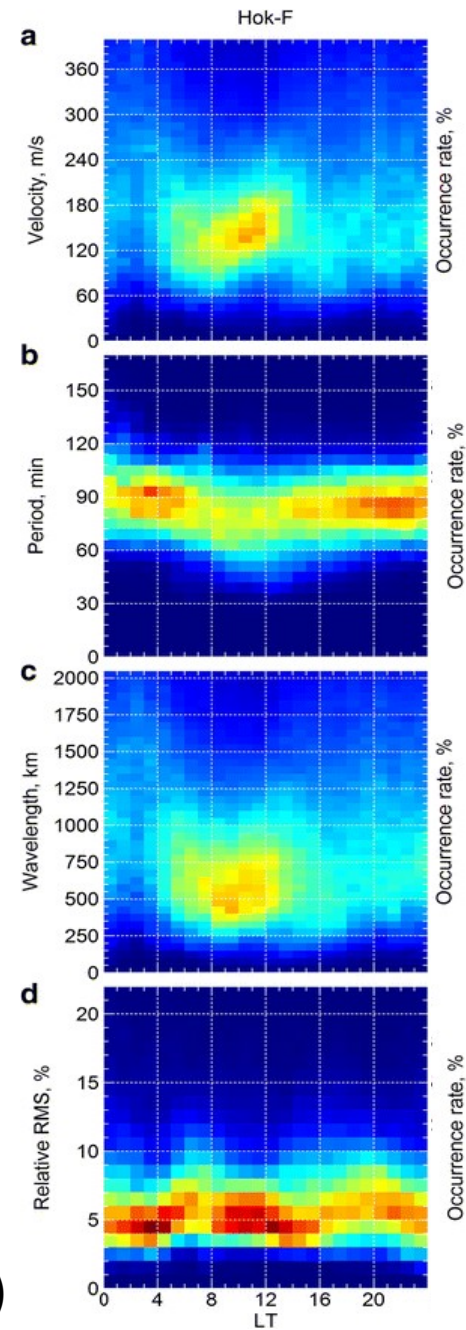
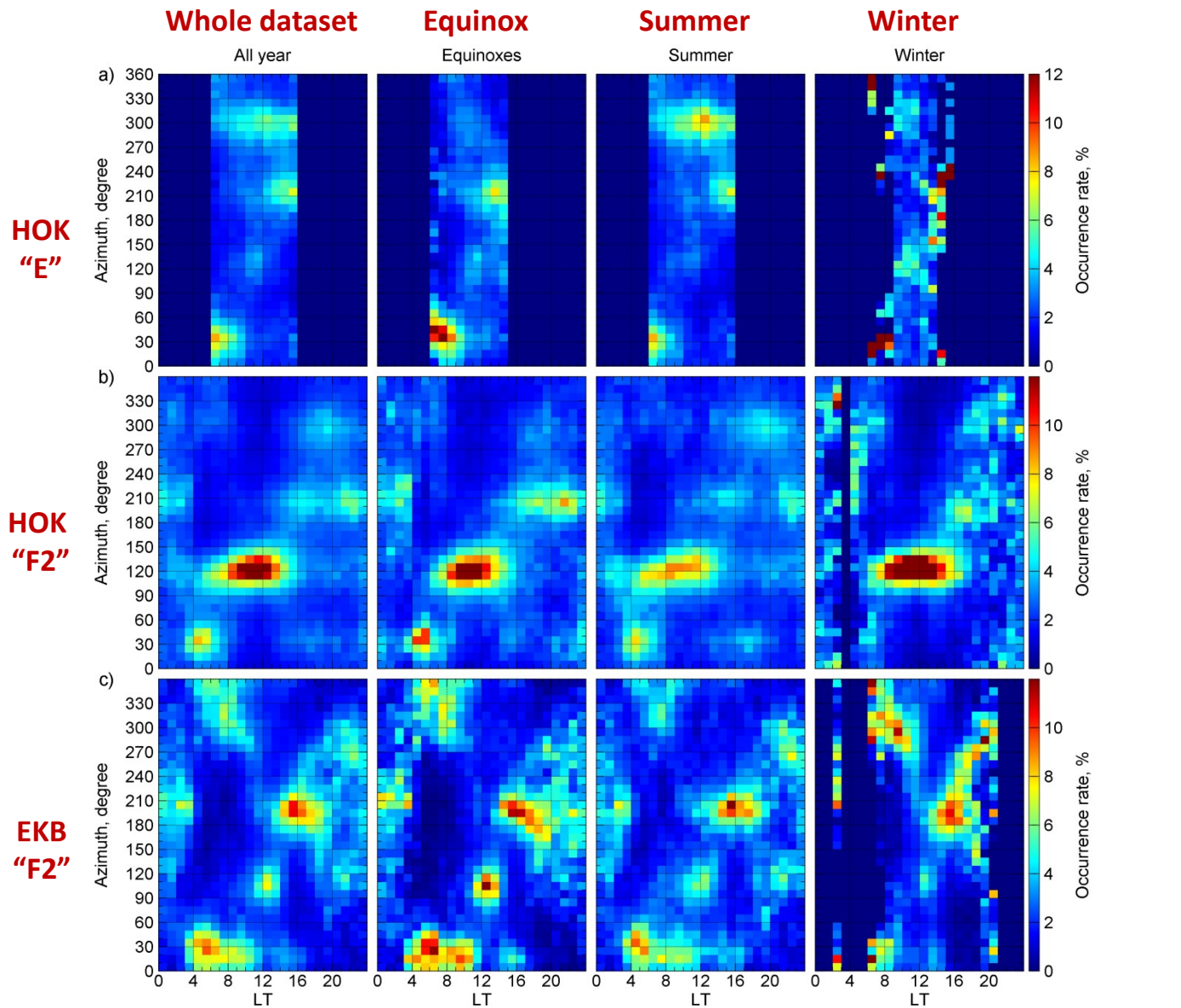


Hokkaido RTI obtained on the beam #0 in November 24, 2011. Red line on the bottom panel is a simulated diurnal variation of minimal range. Black lines is a corresponding “mask” for correct minimal range variations extraction.

Determined diurnal dependencies of azimuth and apparent horizontal velocity and corresponding distributions



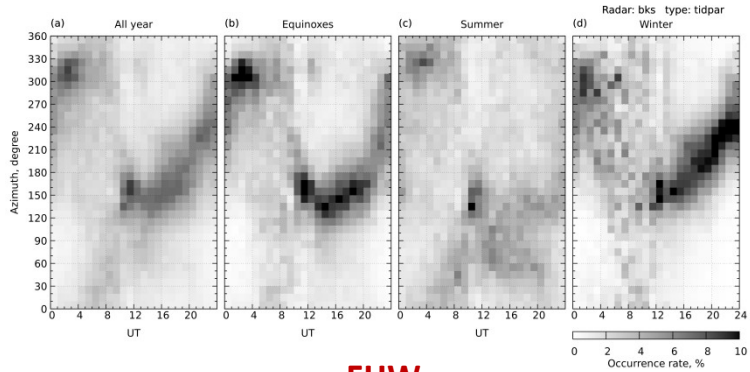
1.2. Statistical study of MSTID's parameters



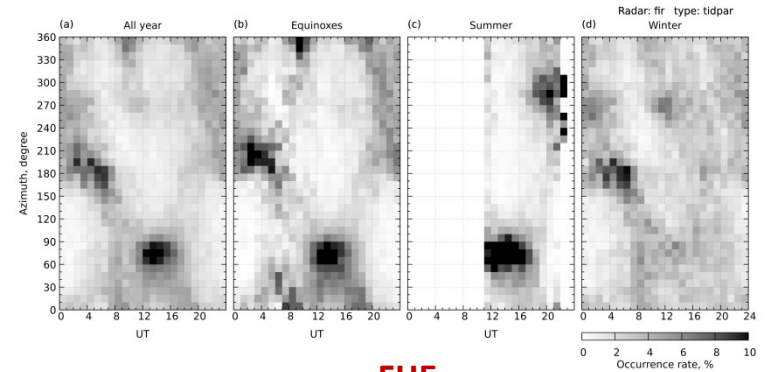
Oinats et al. (2016)

1.2. Statistical study of MSTID's parameters

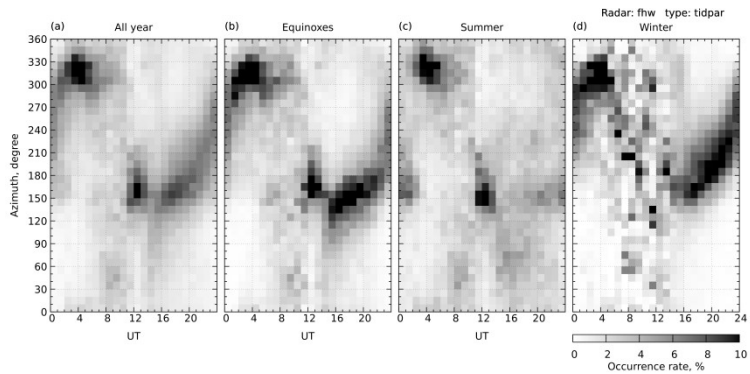
BKS



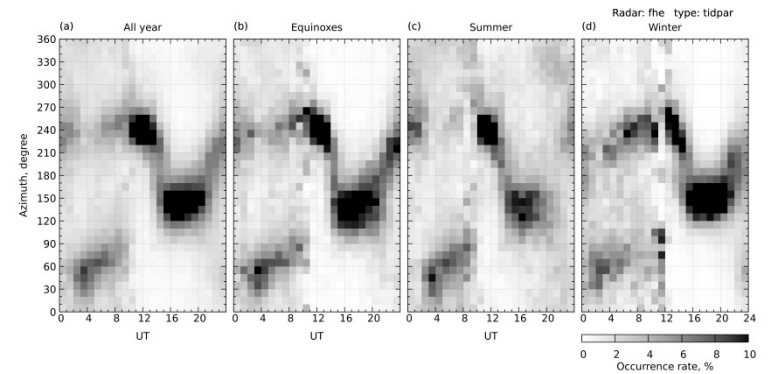
FIR



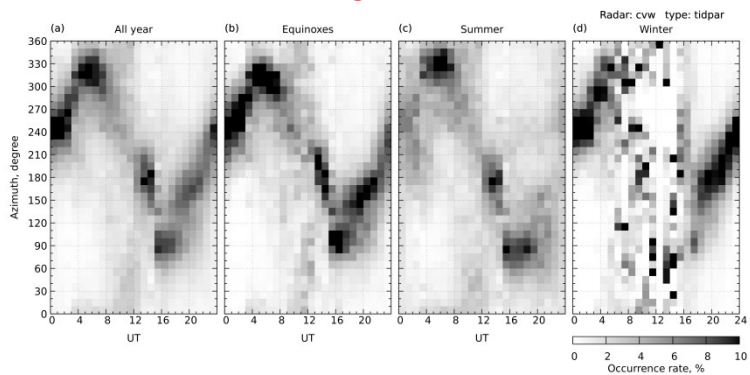
FHW



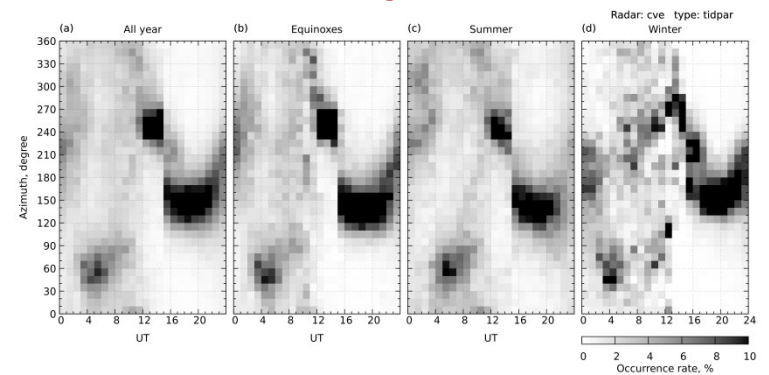
FHE



CVW



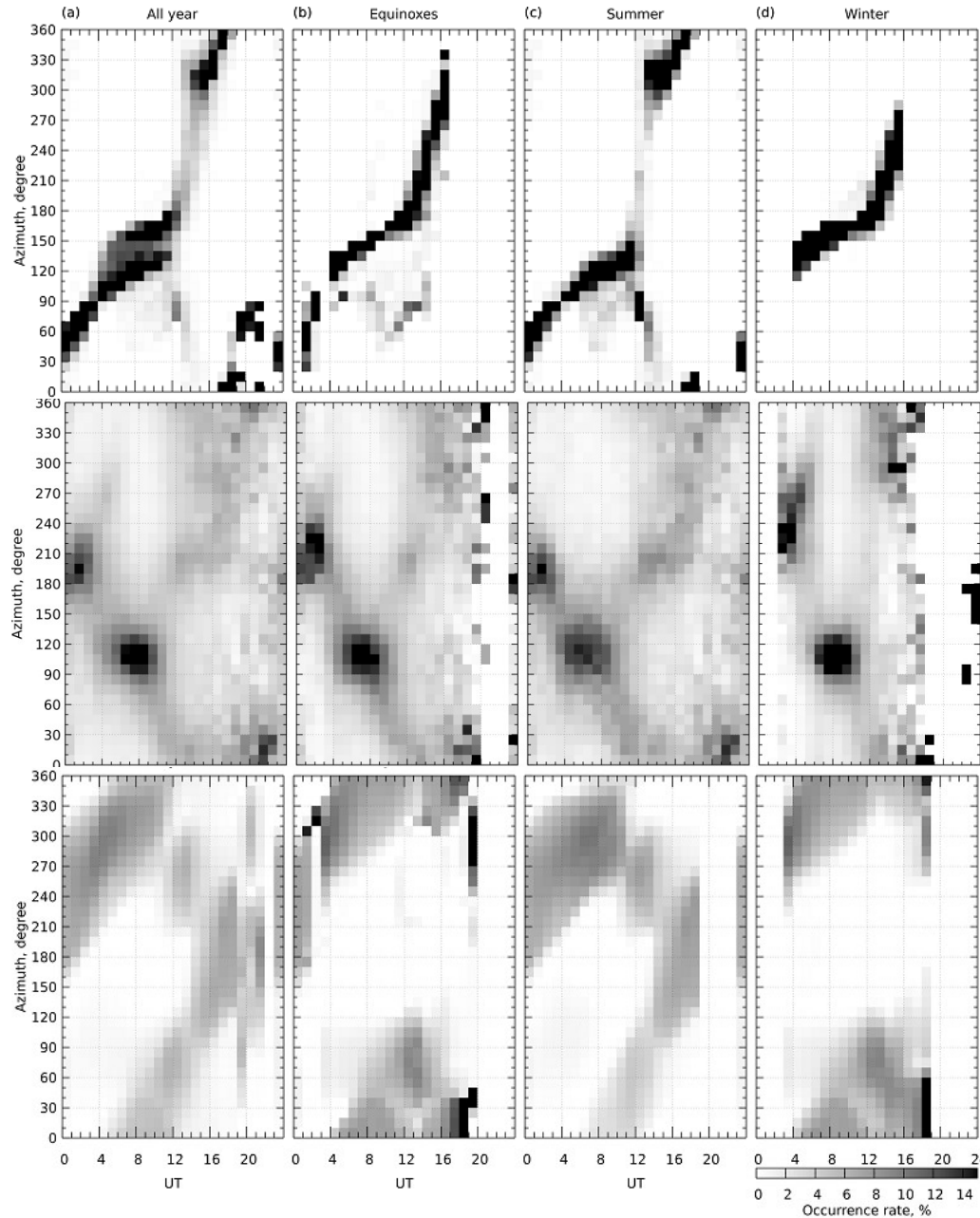
CVE



*preliminary results

1.3. Comparison with neutral wind models

**EKB
(2013 - 2021)**



**“Allowed”
azimuths
(HWM14)**

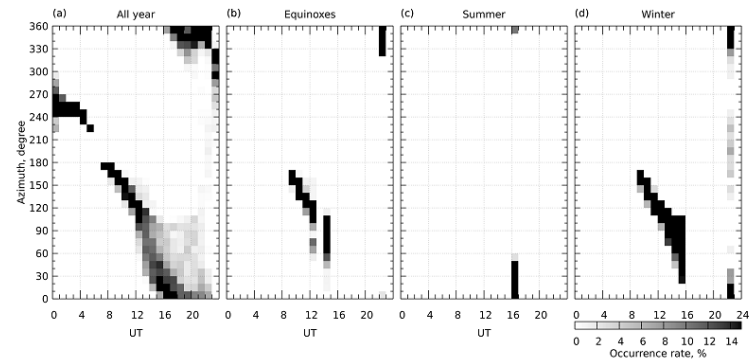
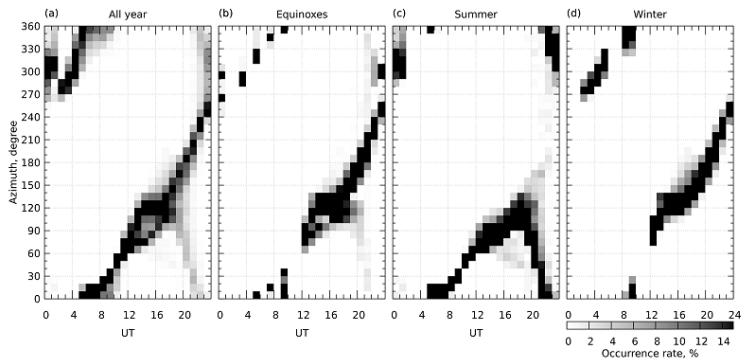
**Observed
MSTID
azimuths**

**“Restricted”
azimuths
(HWM14)**

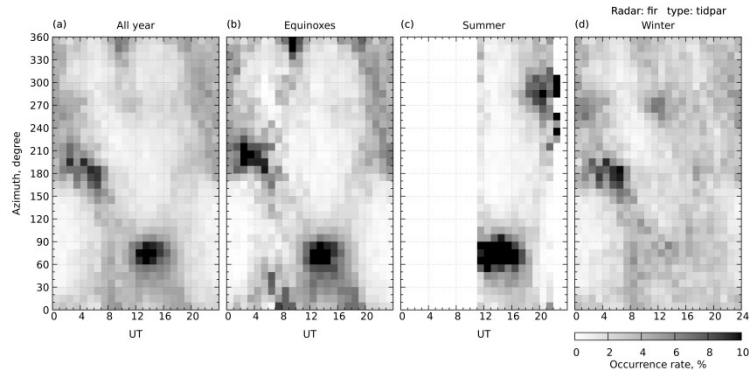
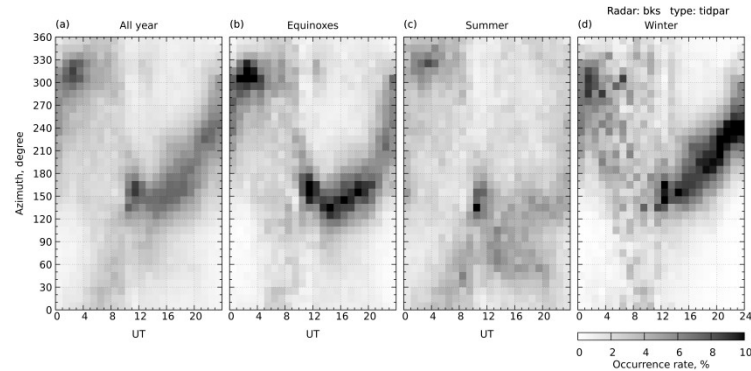
1.3. Comparison with neutral wind models

BKS (2010-2011 and 2013-2014)

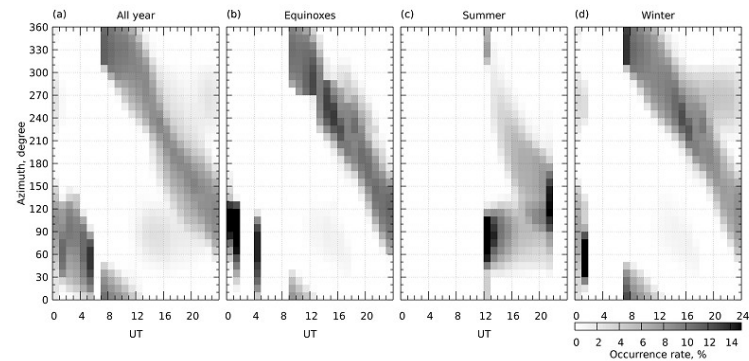
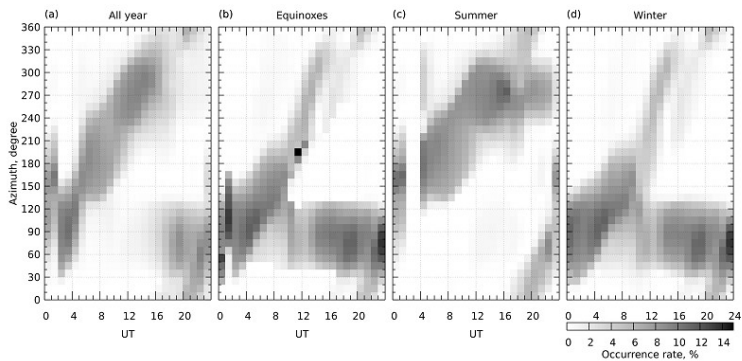
FIR (February 2010 – October 2011)



**“Allowed”
azimuths
(HWM14)**



**Observed
MSTID
azimuths**



**“Restricted”
azimuths
(HWM14)**

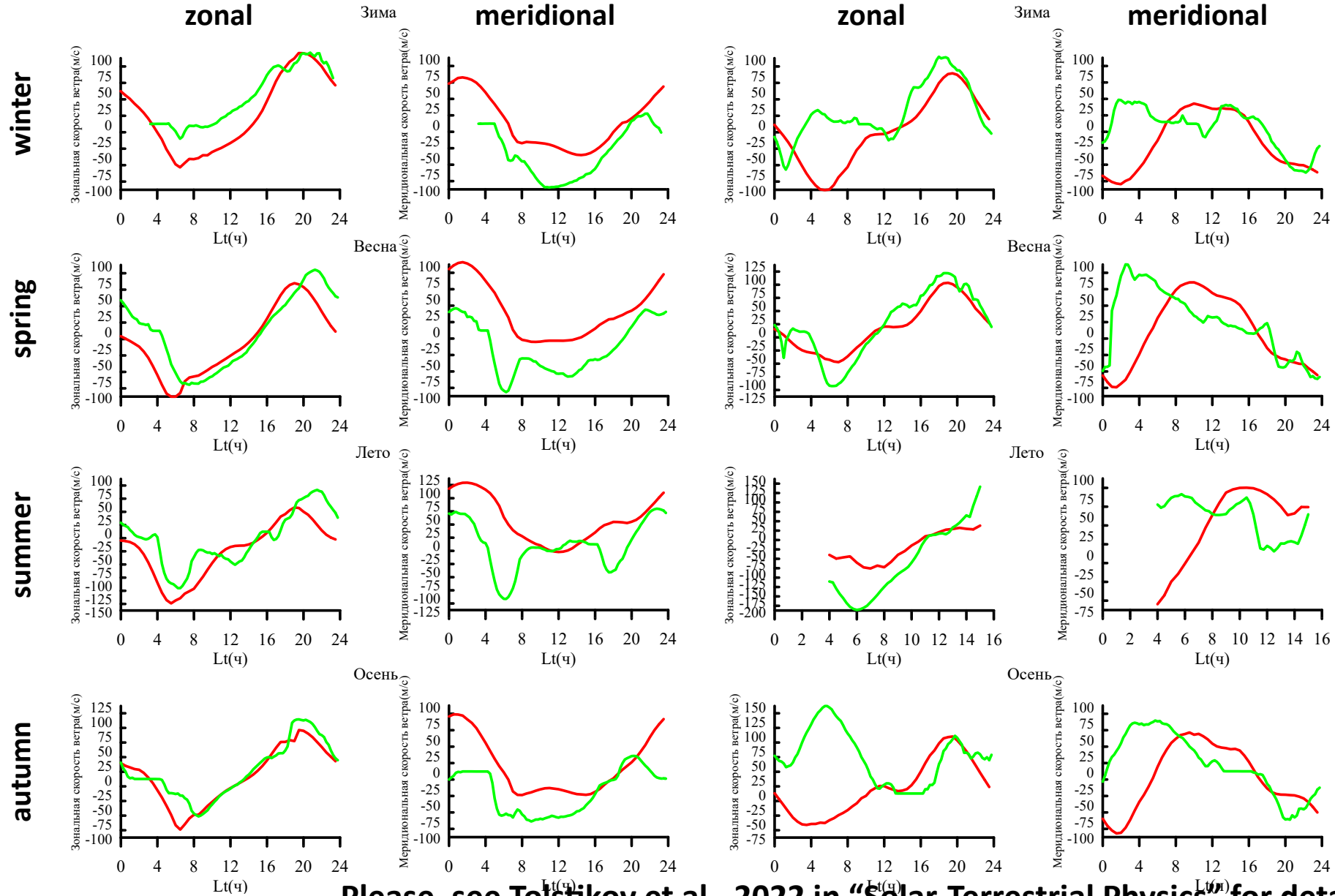
1.3. Comparison with neutral wind models

GREEN – calculated

RED – HWM14

BKS (2010-2011 and 2013-2014)

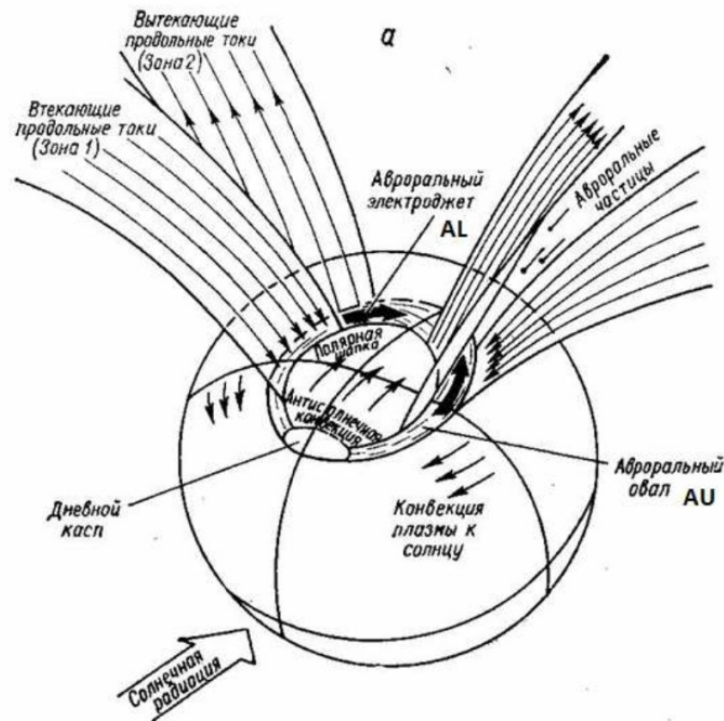
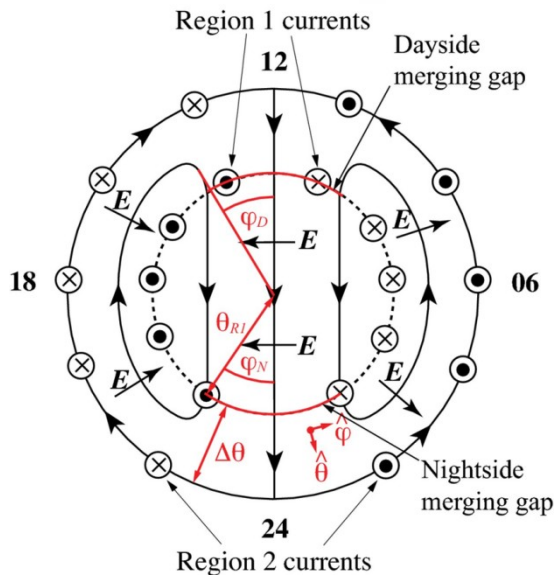
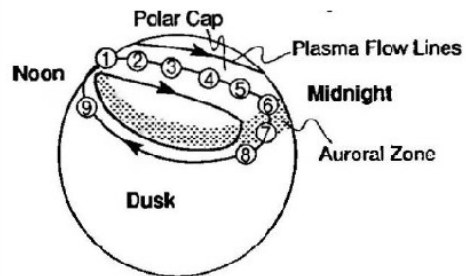
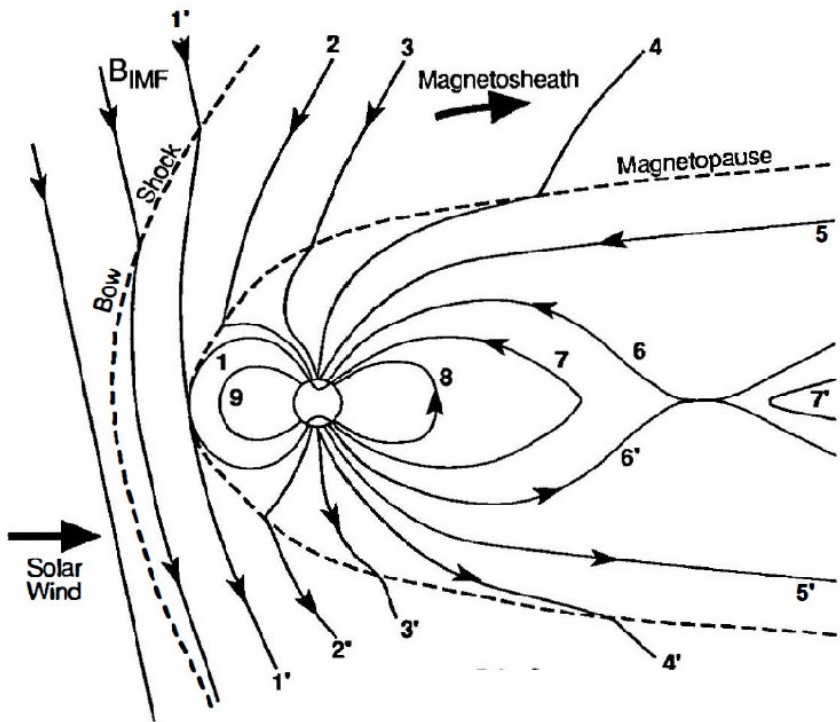
FIR (February 2010 – October 2011)



Please, see Tolstikov et al., 2022 in "Solar-Terrestrial Physics" for details

2. Field-aligned irregularities (FAI). GDI growth rate

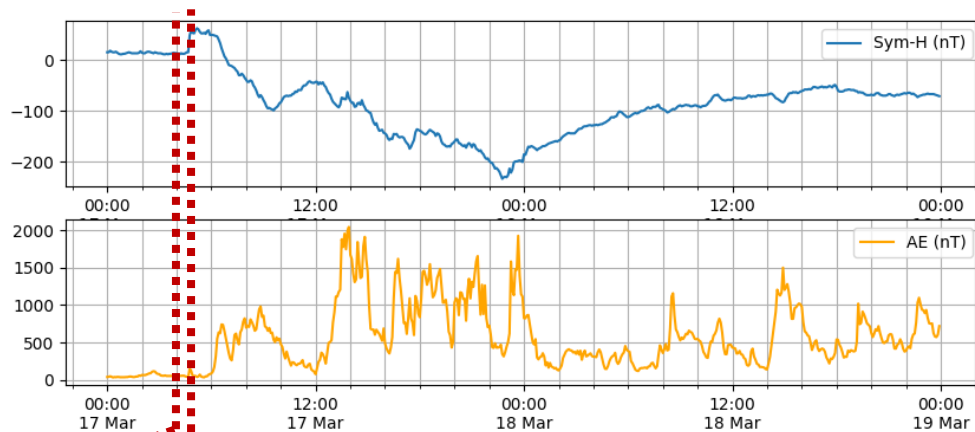
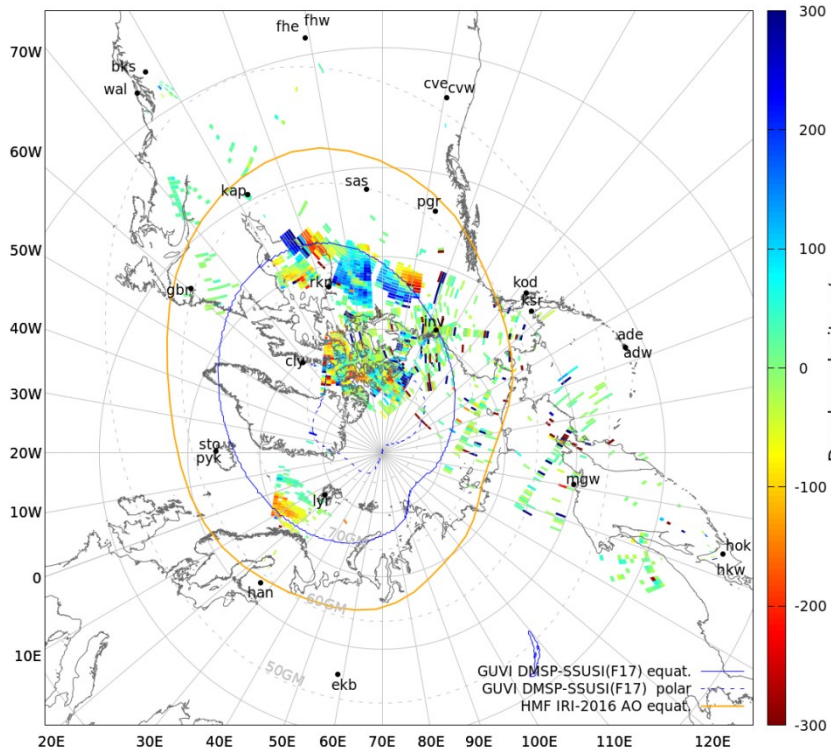
(Dungey, 1961)



2. Field-aligned irregularities (FAI). GDI growth rate

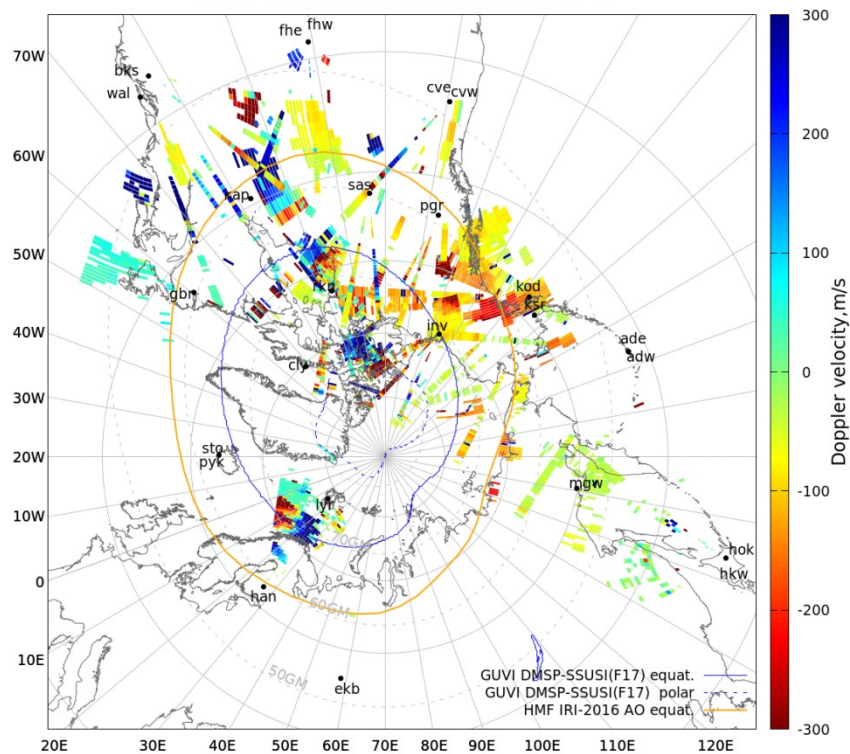
04:44UT 17.05.2015

NH HF radars data [2015.03.17 04.44UT]



04:47UT 17.05.2015

NH HF radars data [2015.03.17 04.47UT]



Sudden storm commencement (SSC) effects during St. Patrick's day superstorm

2. Field-aligned irregularities (FAI). GDI growth rate

Gradient-drift instability (GDI) growth rate in the ionospheric F region
[Makarevich, 2014]

$$\gamma^F \cong \frac{\mathbf{k} \cdot \hat{\mathbf{b}} \times \mathbf{G}}{1 + \psi} \frac{1}{k^2} \frac{\mathbf{k} \cdot \mathbf{E}_0}{B} = \frac{GV_E}{1 + \psi} (\hat{\mathbf{k}} \cdot \hat{\mathbf{b}} \times \hat{\mathbf{g}}) (\hat{\mathbf{k}} \cdot \hat{\mathbf{e}})$$



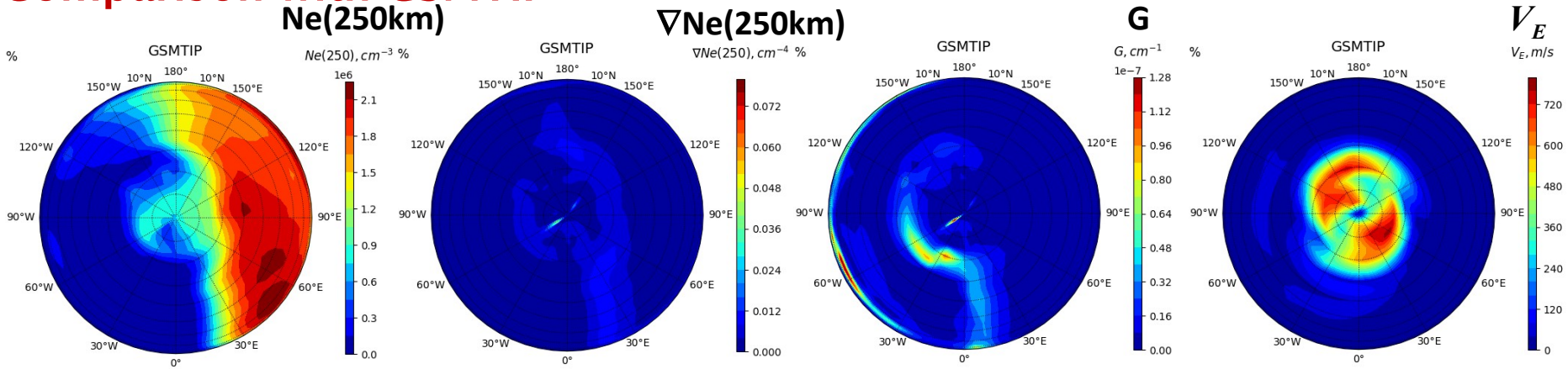
$$\gamma^F = -\frac{GV_E}{1 + \psi} \cos \alpha \cos (\alpha - \beta)$$

The angles give orientation of GDI wave vector and electric field in the XY plane when use a coordinate system with axes directed along the electron density gradient vector (Oy) and magnetic field (Oz)

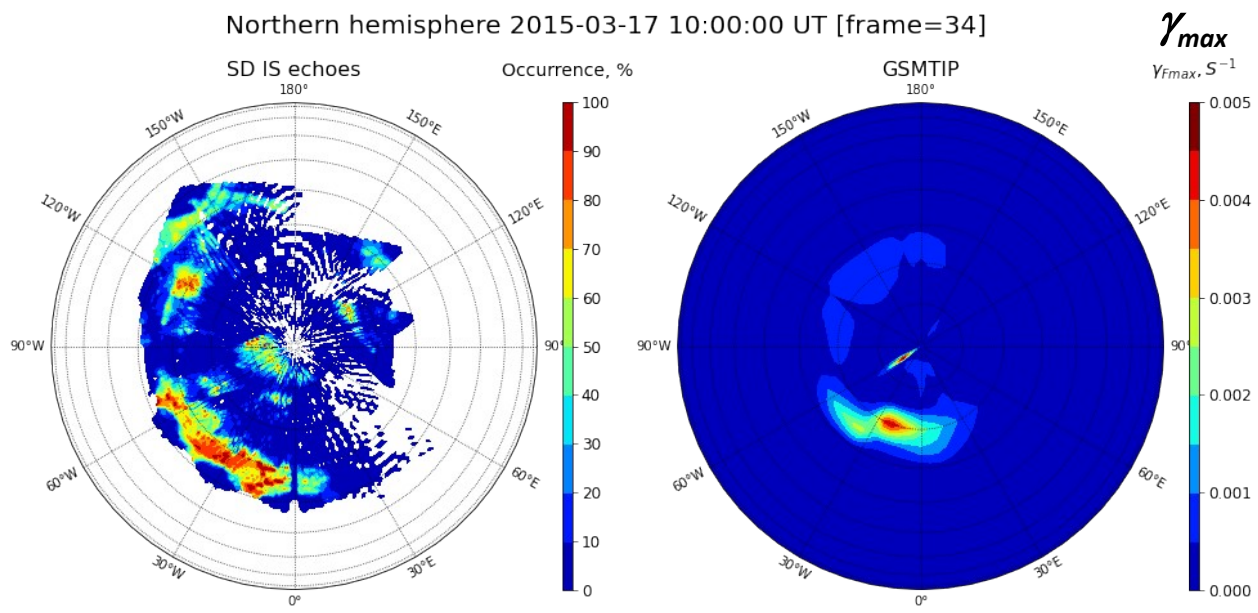


$$\gamma_{\max}^F = -GV_E$$

2.1. FAI observation during St.Patrick superstorm (March 17-18, 2015). Comparison with GSMTIP



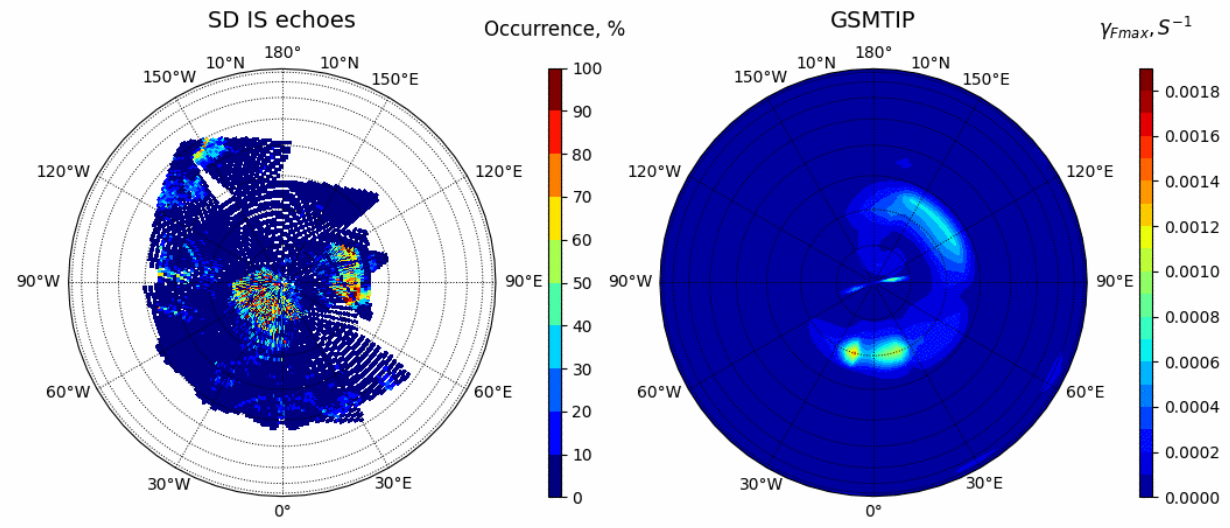
Please, see details about GSMTIP in [Korenkov et al., 1998; Klimenko et al., 2019]



2.1. FAI observation during St.Patrick superstorm (March 17-18, 2015). Comparison with GSMTIP

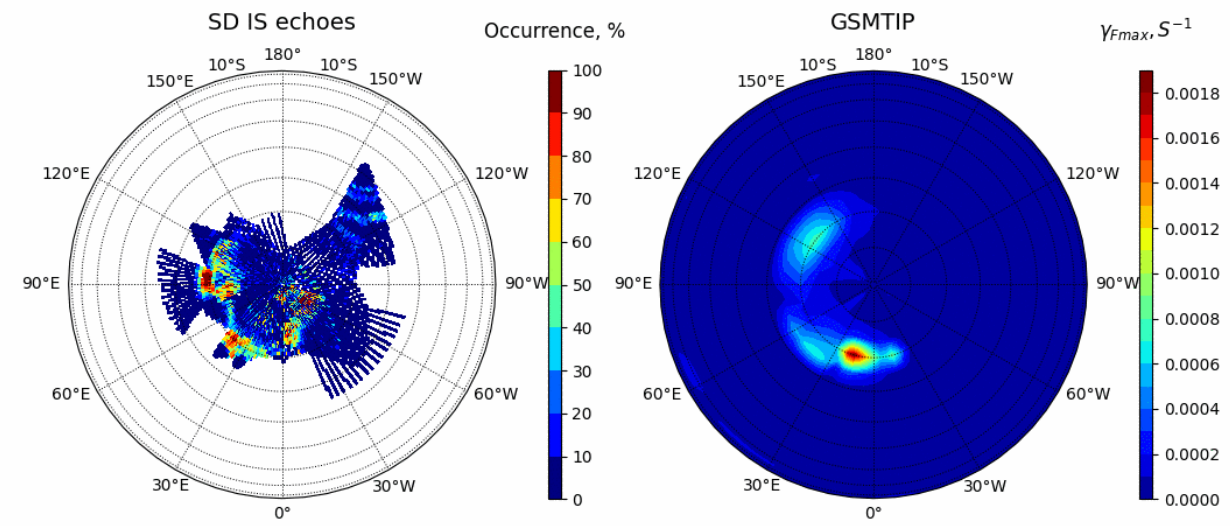
Northern hemisphere 2015-03-16 00:00:00 UT

NH



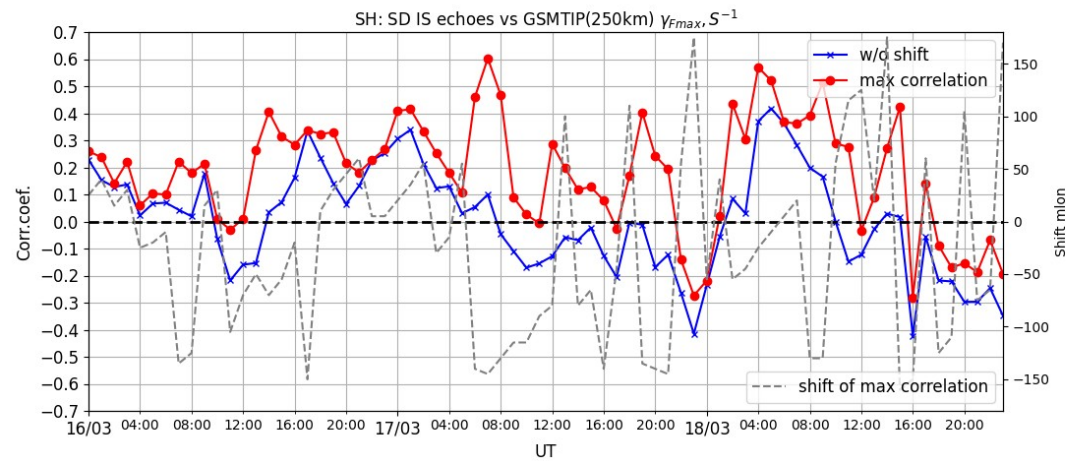
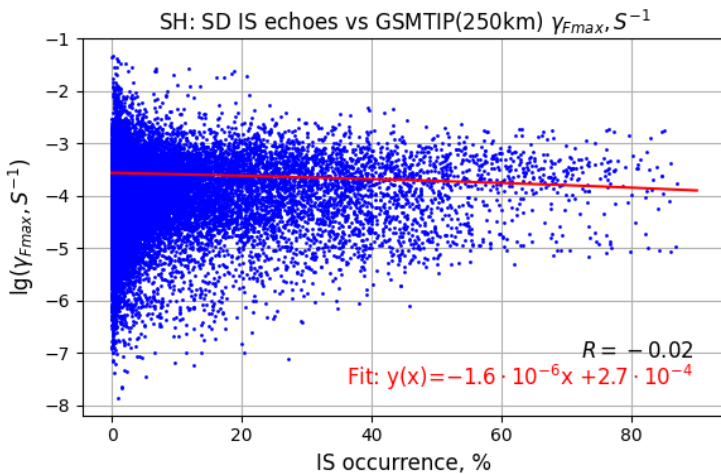
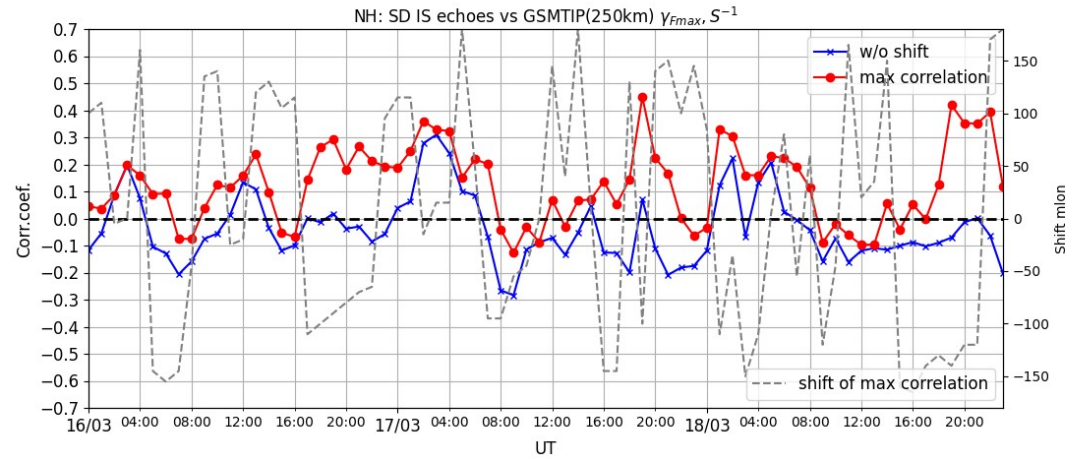
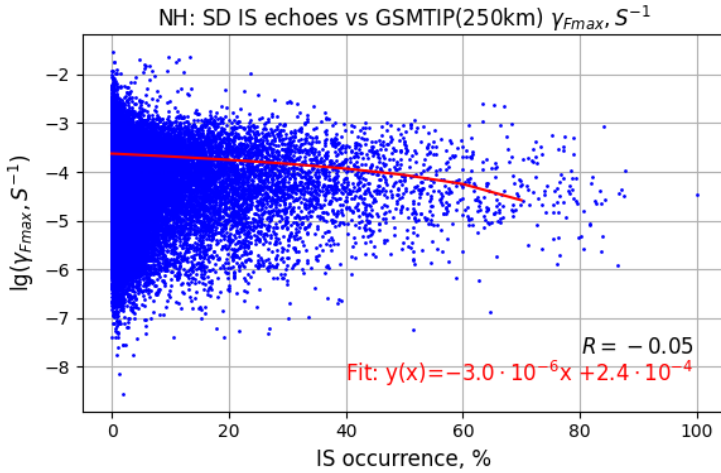
Southern hemisphere 2015-03-16 00:00:00 UT

SH



2.1. FAI observation during St.Patrick superstorm (March 17-18, 2015). Comparison with GSMTIP

GSMTIP – regression and correlation



2.1. FAI observation during St.Patrick superstorm (March 17–18, 2015). Comparison with GSMTIP

GSMTIP, GDMF2, IRI2020 – regression and correlation

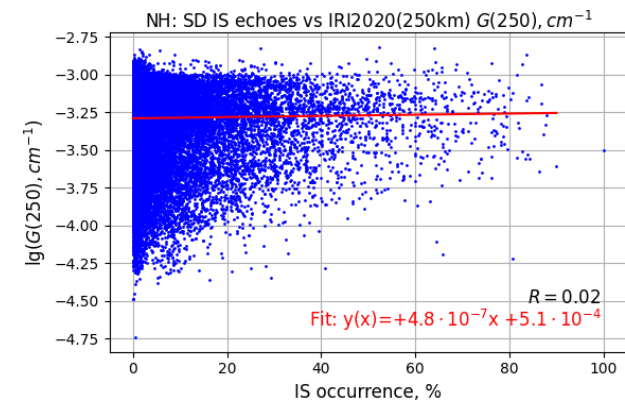
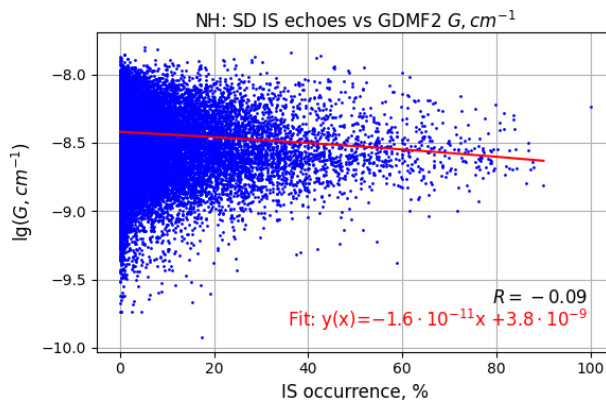
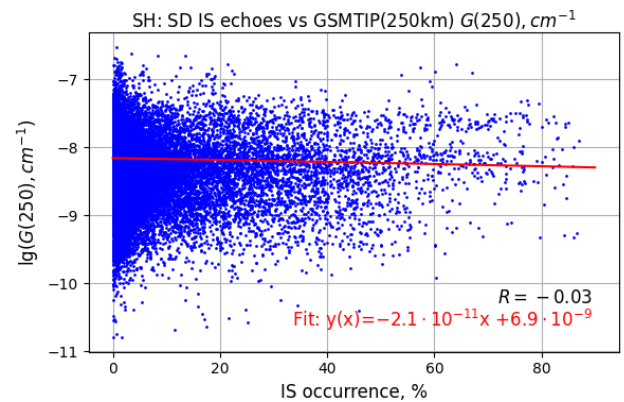
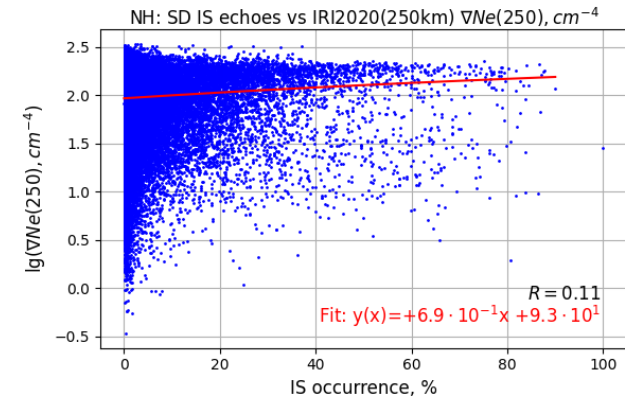
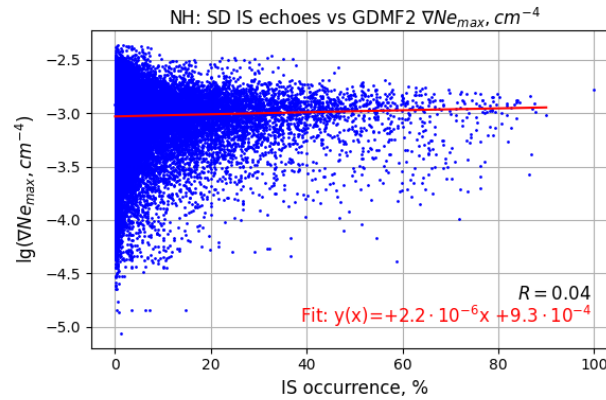
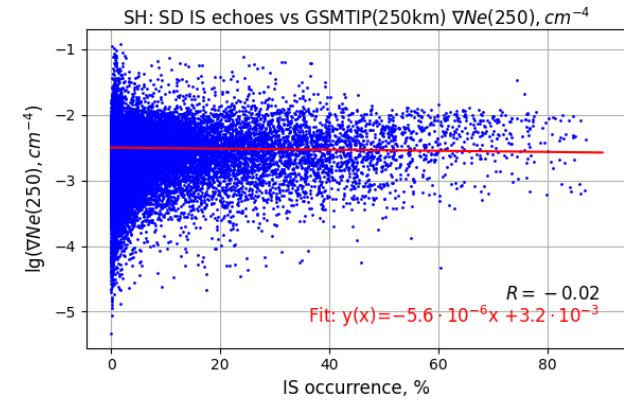
GSMTIP

GDMF2

IRI2020

[Shubin & Deminov, 2019]

[Bilitza et al., 2022]

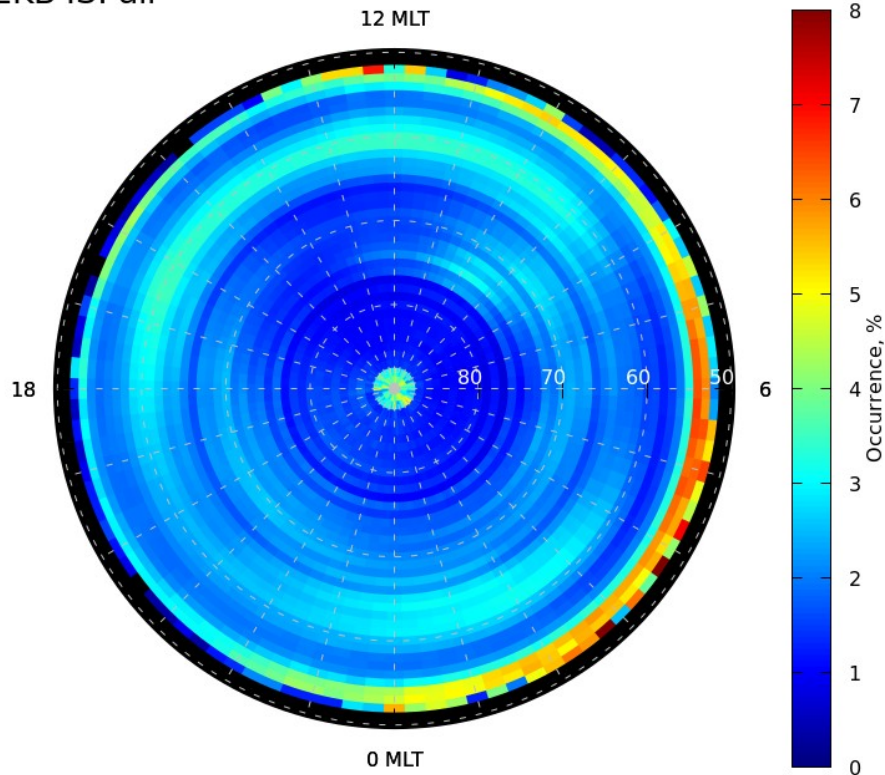


2.1. FAI observation during St.Patrick superstorm (March 17–18, 2015). Comparison with GSMTIP

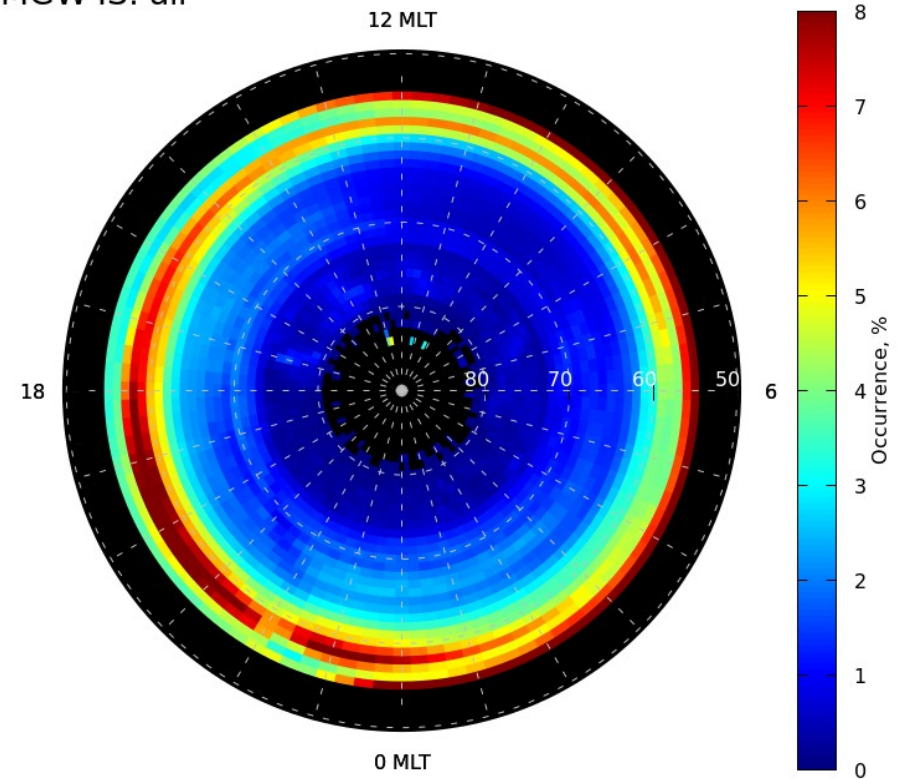
Dataset	Ne_{max}	∇Ne	G	γ_{max}
	GSMTIP			
NH	-0.09	-0.07	-0.04	-0.05
SH	0.07	-0.05	-0.05	-0.02
GDMF2				
NH	0.12	0.04	-0.09	
SH	-0.07	-0.05	0.03	
IRI2020				
NH	0.12	0.05	-0.07	
SH	-0.02	-0.04	-0.06	

2.2. Statistical study of FAI occurrence observed by EKB and MGW radars

EKB IS: all



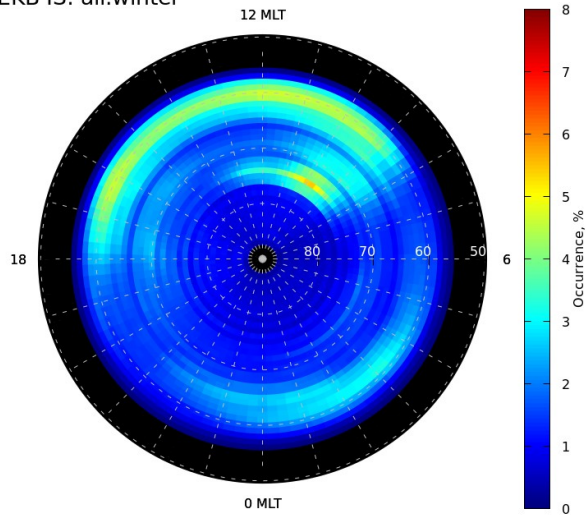
MGW IS: all



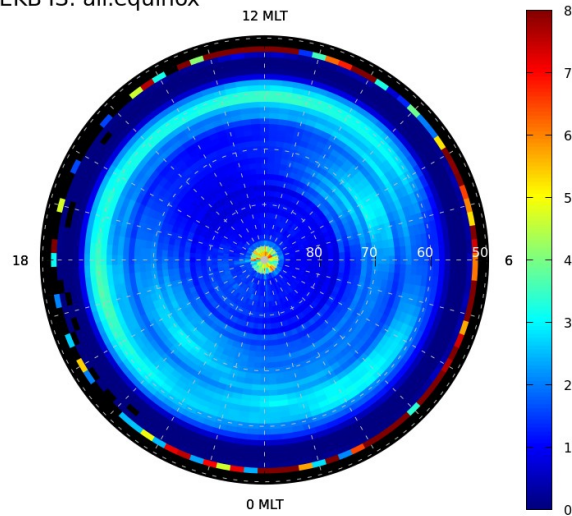
2.2. Statistical study of FAI occurrence observed by EKB and MGW radars

Seasonal dependence

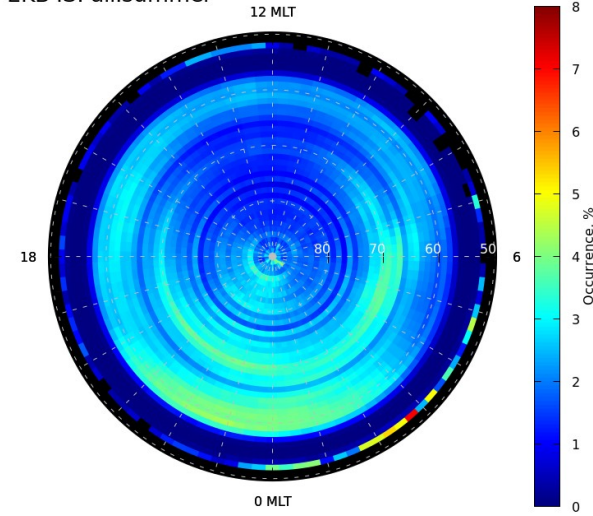
EKB IS: all.winter



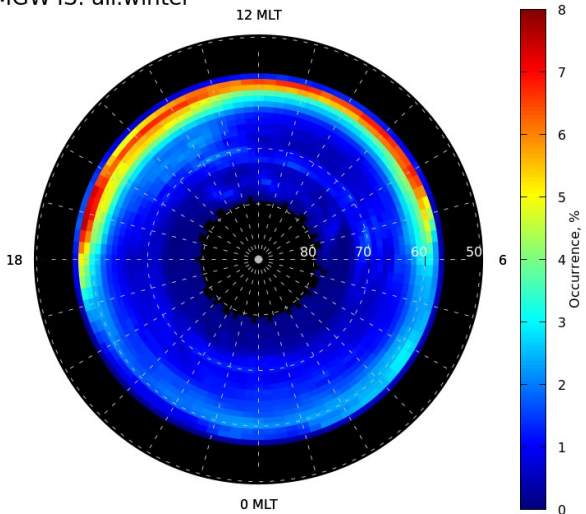
EKB IS: all.equinox



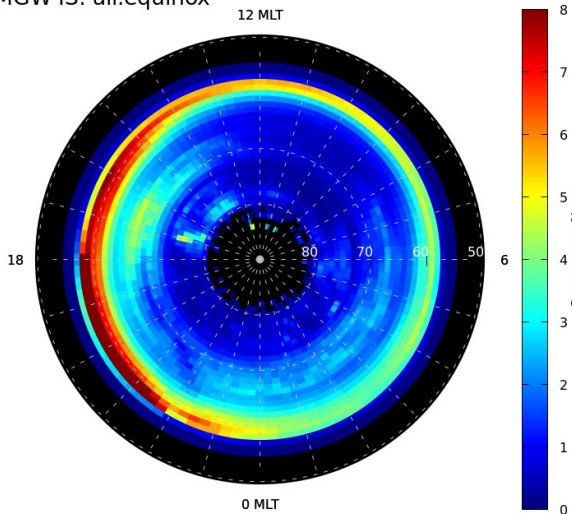
EKB IS: all.summer



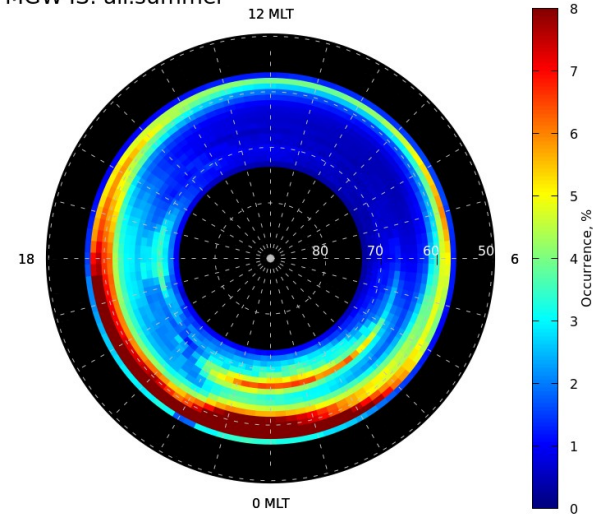
MGW IS: all.winter



MGW IS: all.equinox

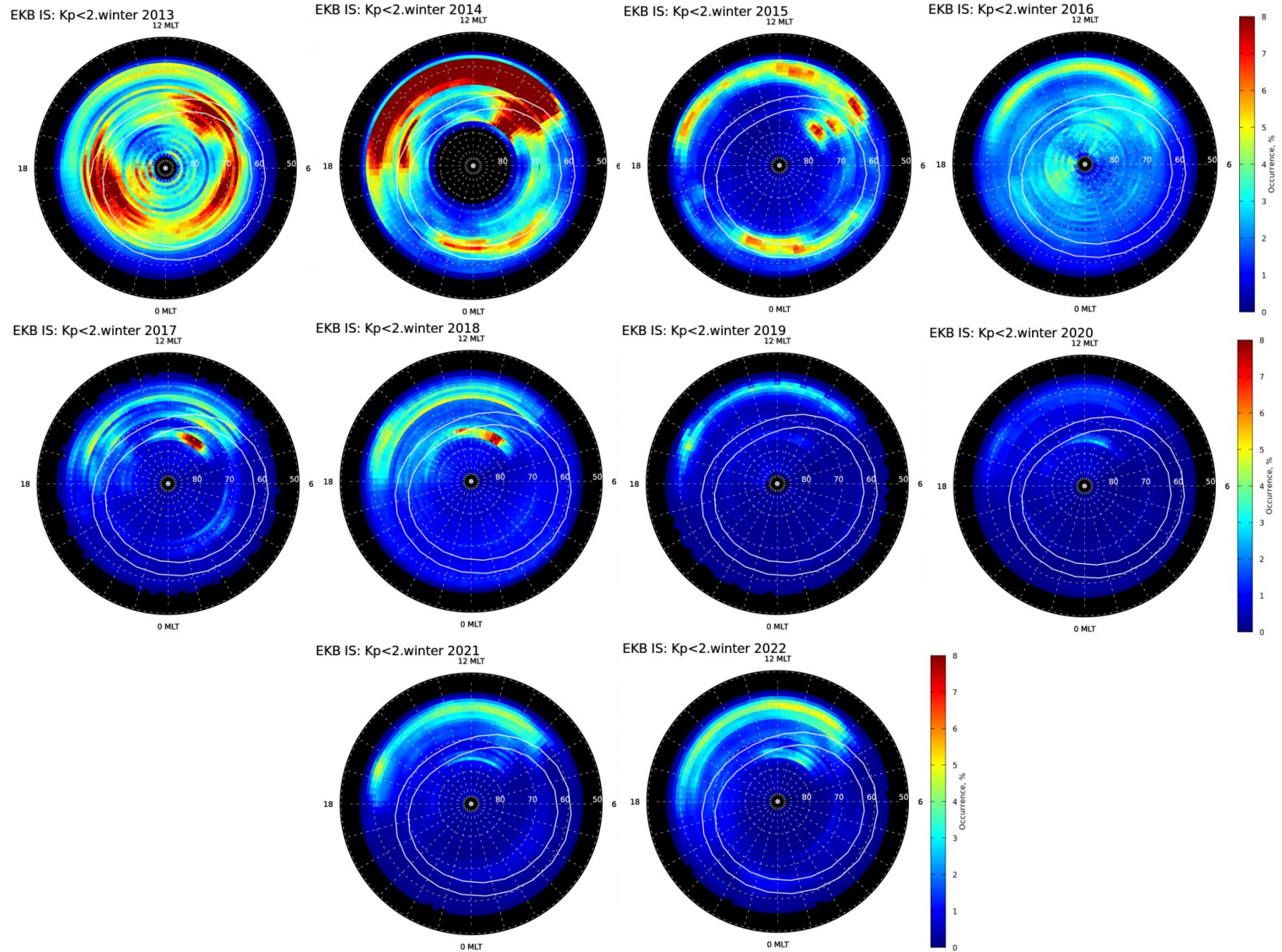


MGW IS: all.summer



2.2. Statistical study of FAI occurrence observed by EKB and MGW radars

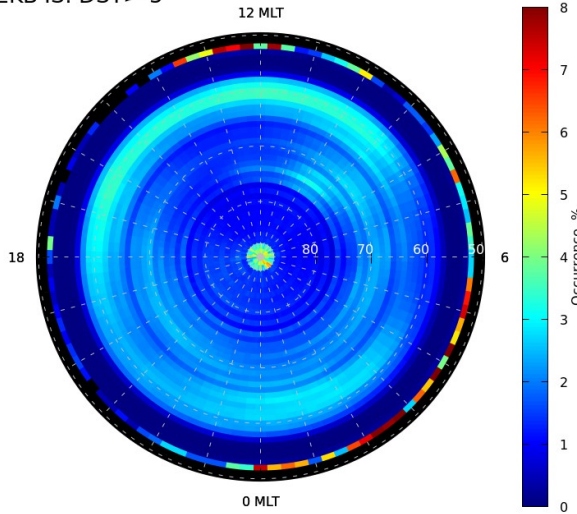
Solar activity dependence



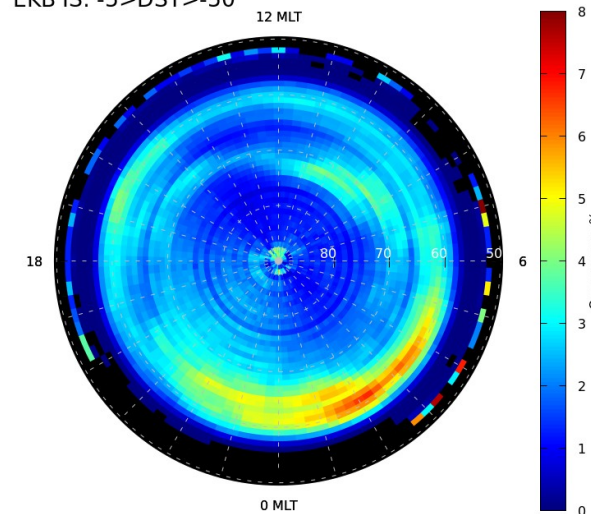
2.2. Statistical study of FAI occurrence observed by EKB and MGW radars

Geomagnetic activity dependence

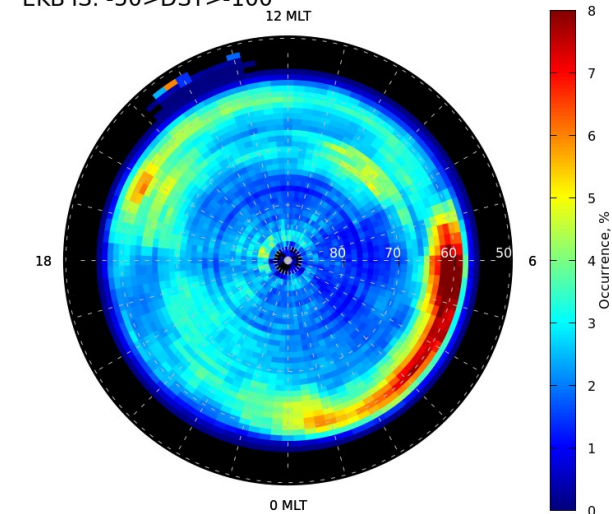
EKB IS: $DST > -5$



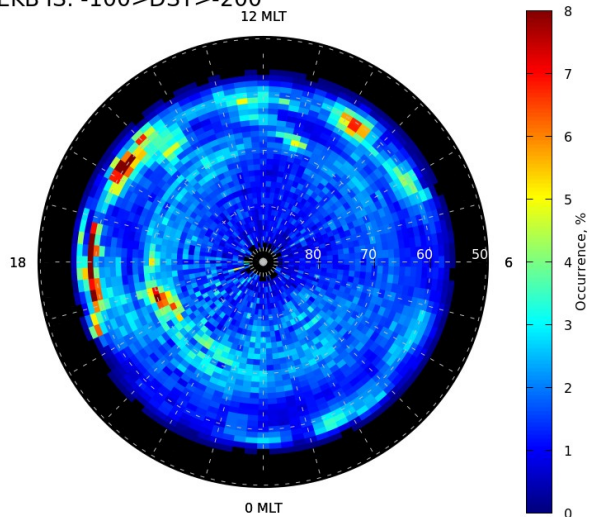
EKB IS: $-5 > DST > -50$



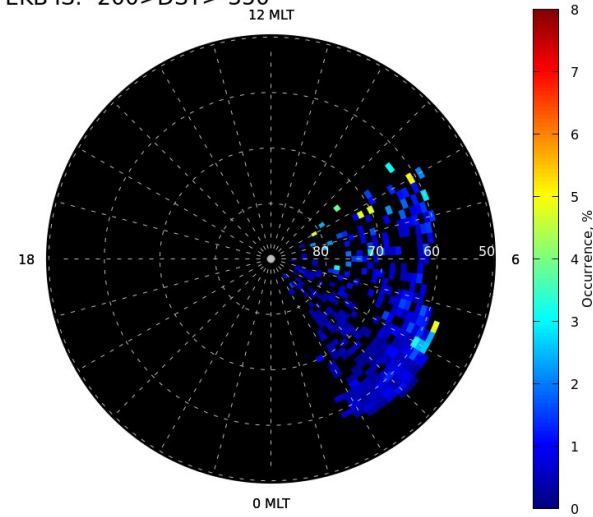
EKB IS: $-50 > DST > -100$



EKB IS: $-100 > DST > -200$

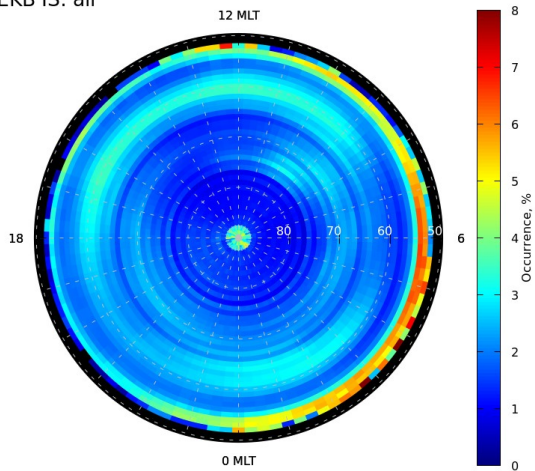


EKB IS: $-200 > DST > -350$

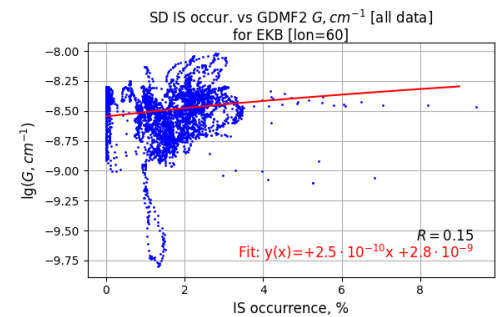
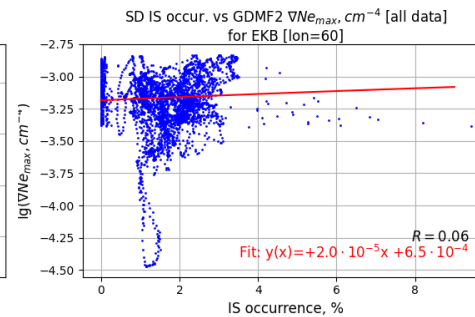
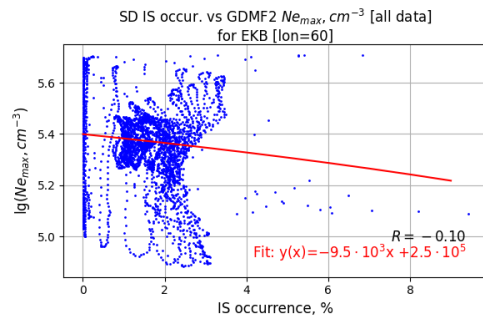
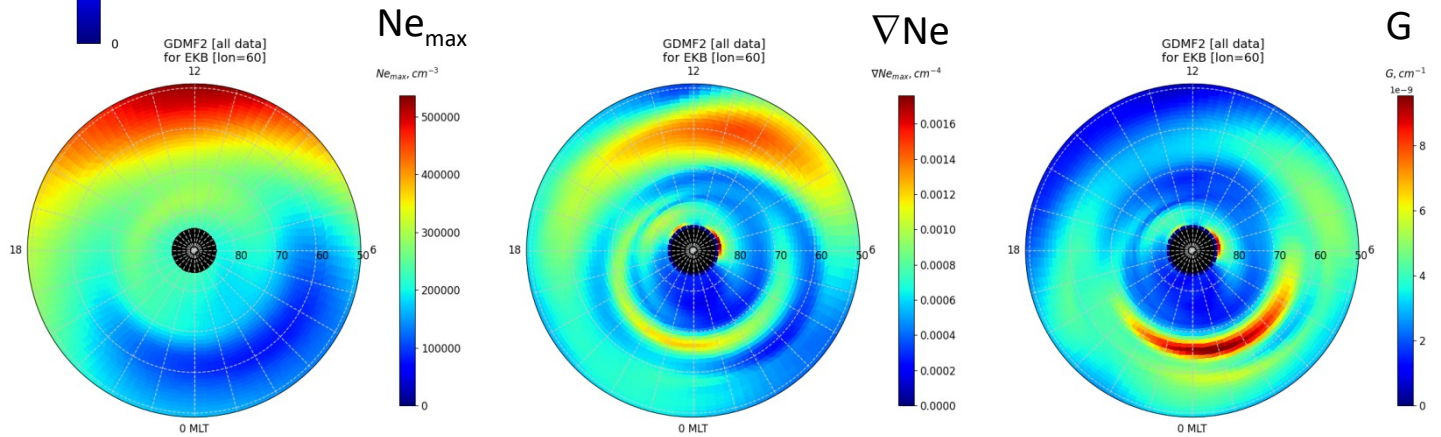


2.3. Comparison with empirical ionosphere models

EKB IS: all

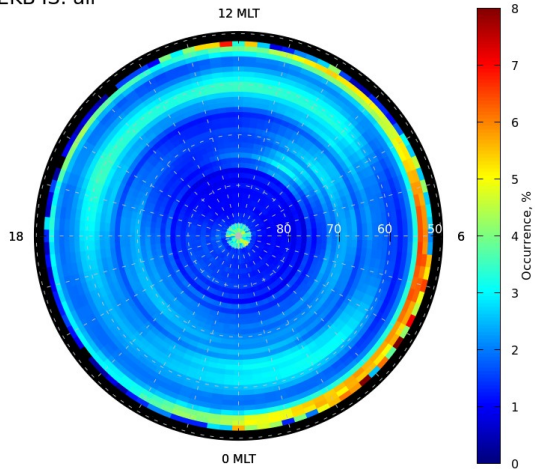


GDMF2

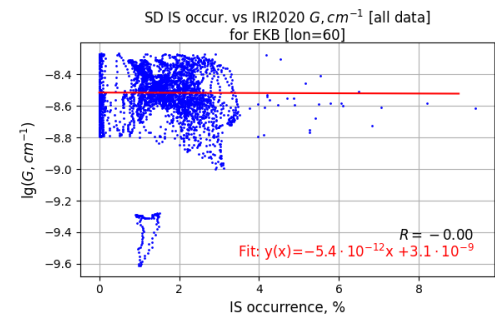
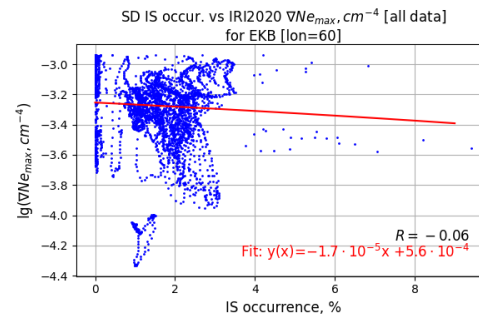
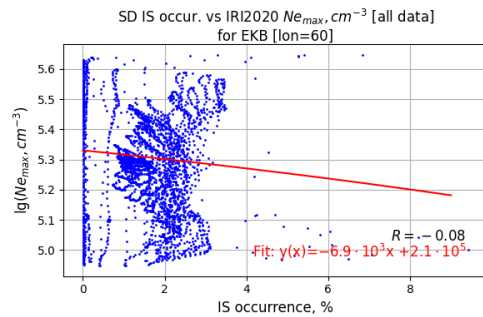
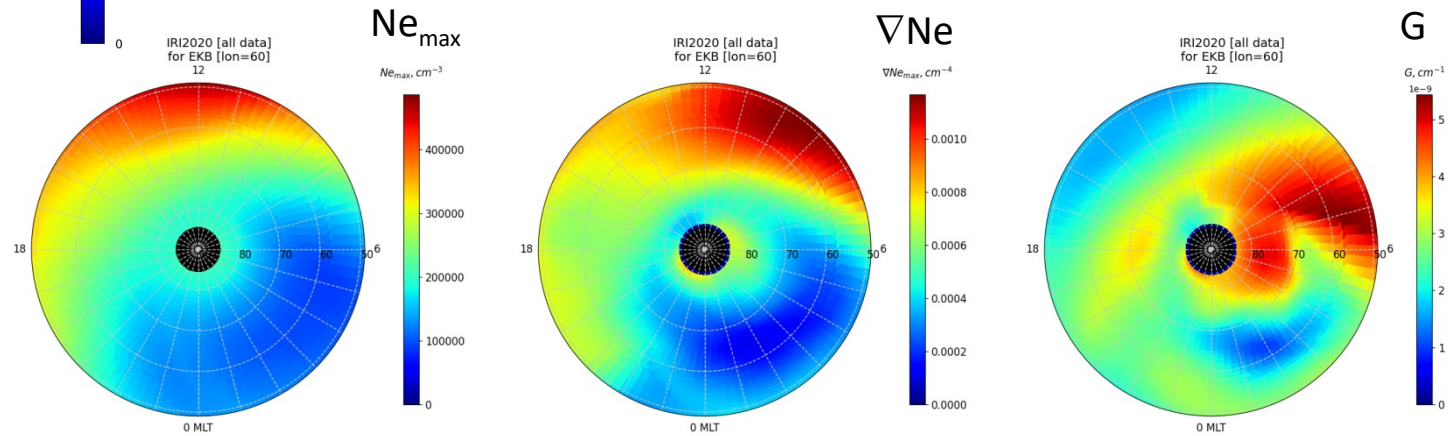


2.3. Comparison with empirical ionosphere models

EKB IS: all



IRI2020



2.3. Comparison with empirical ionosphere models

Dataset	GDMF2			IRI2020		
	Ne_{max}	∇Ne	G	Ne_{max}	∇Ne	G
All data	-0.1/-0.07*	0.06/ 0.38 *	0.15/0.4*	-0.08/0.1*	-0.06/0.07*	0.0/-0.24*
Winter	0.32/0.35*	0.49/ 0.52 *	0.21/0.17*	0.36/0.45*	0.43/0.42*	0.22/0.12*
Summer	-0.41/0.15*	-0.11/ 0.49 *	0.06/0.56*	-0.38/0.1*	-0.21/0.41*	-0.04/0.44*
Equinox	-0.04/-0.01*	0.04/ 0.39 *	0.09/0.32*	-0.03/0.12*	-0.05/0.04*	-0.04/-0.13*
Kp<2	-0.36/0.02*	0.08/ 0.36 *	-0.02/0.35*	0.05/0.12*	0.09/0.09*	0.06/-0.21*
2<=Kp<3	0.08/-0.08*	0.08/0.38*	0.22/ 0.42 *	-0.07/0.09*	-0.07/0.03*	-0.06/-0.3*
Kp>=3	-0.12/-0.09*	-0.06/ 0.29 *	0.21/0.27*	-0.25/0.1*	-0.25/0.05*	-0.13/-0.2*
2013	0.04	0.09	-0.02	-0.04	0.07	0.25
2014	0.51	0.59	0.07	0.55	0.59	0.34
2015	0.18	0.38	0.39	0.18	0.23	0.2
2016	0.34	0.15	-0.36	0.27	0.36	0.34
2017	0.30	0.23	-0.14	0.26	0.40	0.31
2018	0.31	0.24	-0.1	0.35	0.37	0.09
2019	0.48	0.38	-0.1	0.52	0.43	-0.03
2020	0.54	0.37	-0.17	0.52	0.46	-0.04
2021	0.55	0.58	-0.07	0.62	0.63	0.13
2022	0.55	0.66	0.07	0.59	0.69	0.37

*EKB/MGW

CONCLUSIONS and FINAL REMARKS

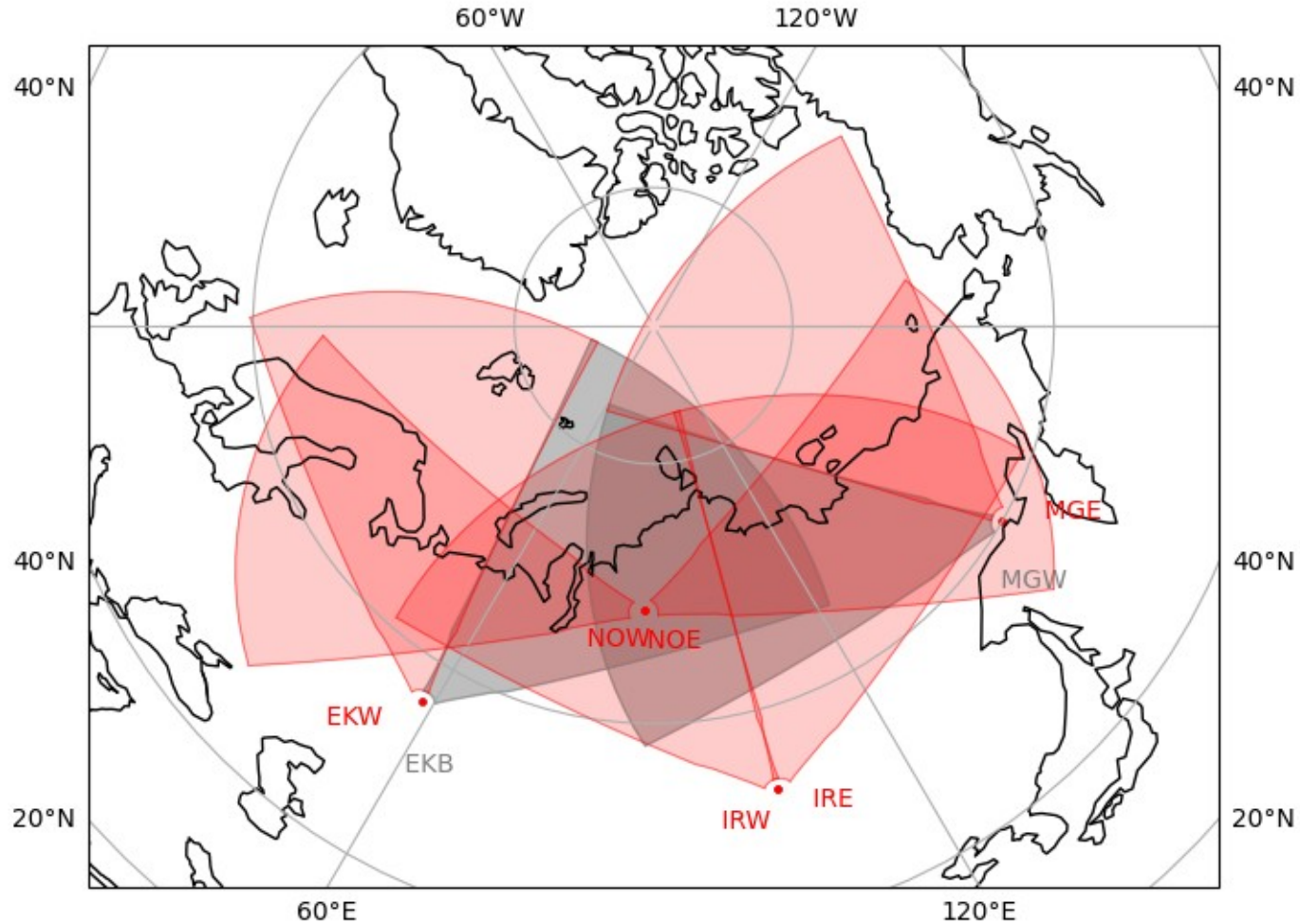
HF radars are very effective tool for monitoring ionospheric dynamics in a wide spatial regions including polar, auroral, sub-auroral, and mid-latitudes.

Statistical dependencies of the main parameters of MSTIDs on the time of day, season of the year, levels of solar and geomagnetic activity, location of HF radars, and the state of the neutral atmosphere are revealed. Properties of most of the MSTIDs are in good agreement with the hypothesis of IGW filtration by neutral wind. This allowed us to develop and test a method for estimating the horizontal neutral wind velocity vector based on statistical distributions of MSTIDs azimuths and velocities.

First principle and empirical ionosphere models allows for a satisfactory prediction of FAI generation regions of, both during individual events and for the purpose of interpreting statistically observed patterns. Monitoring of radio aurora in quiet and disturbed conditions is useful for validating the models of large-scale ionospheric formations, such as the MIT, auroral oval, SAPS, SAID, etc. Location and dynamics of the aspect scattering regions are directly related to the radial current systems of the magnetosphere (FAC), and, at the same time, there are features of their manifestation associated with the conditions of radio wave propagation in the absorbing medium.

CONCLUSIONS and FINAL REMARKS

RUSSIAN “SEKIRA” HF RADAR NETWORK (NATIONAL HELIOGEOPHYSICAL COMPLEX OF RAS)



OPERATING PLANNING



THANK YOU FOR ATTENTION!

The work was supported by the Ministry of Science and Higher Education of the Russian Federation. The results were obtained using the equipment of Shared Equipment Center “Angara” [<http://ckp-angara.iszf.irk.ru/>]. The authors acknowledge the use of SuperDARN data. SuperDARN is a collection of radars funded by national scientific funding agencies of Australia, Canada, China, France, Italy, Japan, Norway, South Africa, United Kingdom and the United States of America.